Impact of Hurricane Ivan in Grand Cayman

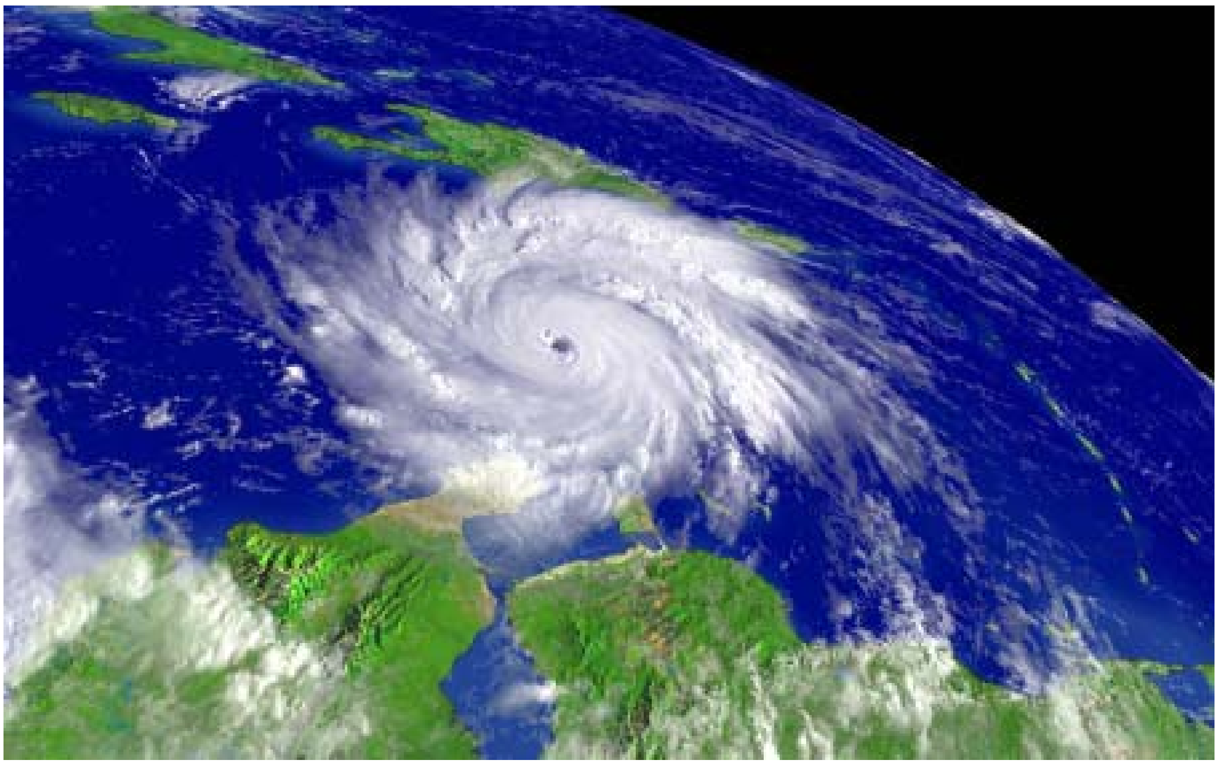

Understanding and quantifying the hazards

Dr Simon R Young
Principal Consultant, GeoSY Ltd

GeoSY Ltd

Prepared by:

Dr Simon R Young
Principal Consultant
GeoSY Ltd

1925 Valleywood Rd & PO Box 224
McLean, VA 22101 Montserrat

Tel/Fax: 703 532 5788
Mobile: 727 709 0008
Email: simon@geosy.com

under contract to:

UK Department for International Development

For Roger Bellers
Disaster Management Advisor for the UK Overseas Territories
South Base, Grand Turk
Turks & Caicos Islands

Submitted: 31 December 2004

GEOSCIENCE AND NATURAL HAZARDS
CONSULTANCY THROUGHOUT THE CARIBBEAN

FRONTISPIECE

A montage of Hurricane Ivan

1 INTRODUCTION

Hurricane Ivan passed close to Grand Cayman on 12 September 2004, buffering the island with strong winds, inducing flooding from storm surge and heavy rain, and causing coastal erosion through enhanced wave action. The sum of these hazardous phenomena produced major damage to roads, utilities and property, especially in the western part of Grand Cayman and along the south coast.

This report presents the results of a detailed scientific study by the author of all available data relating to the severity of the hazards encountered on Grand Cayman during the passage of Ivan. As such, it forms one of two companion reports, the other concentrating on the impact of the hazardous phenomena on the built infrastructure on Grand Cayman and written by Tony Gibbs. A single summary report which merges these two detailed reports, along with a data CD-ROM, act as the final output for this DFID-sponsored project.

Tropical cyclone impacts on the scale of that which occurred in Grand Cayman (and in Grenada) from Hurricane Ivan are fortunately quite rare in the Caribbean, and none has previously affected an island with such well-developed infrastructure and well-enforced building codes. And, although on-the-ground measurements were unfortunately not made as reliably as hoped, various new techniques for characterising tropical cyclones enable a more accurate picture of the storm to be painted than was possible even a few years ago.

The aim of this report is to analyse all of the available data pertaining to the four principal hazardous agents of a tropical cyclone, namely wind, rain, storm surge and wave action. The analysis results in a comprehensive, scientifically defensible hazard profile for Ivan on Grand Cayman, which acts as a foundation for analysing infrastructure damage and economic impacts. The author is not aware of any other study of this detail having been undertaken in the Caribbean following passage of a major hurricane; in fact, it is rare even for a reliable maximum wind speed estimate to be available.

Most of the quantitative data for this study was collected via electronic means; sources included public domain data at the National Hurricane Center and sister NOAA bodies and at various universities in the USA as well as ongoing research outputs from various sources. Qualitative data was also collected electronically but proved to be highly unreliable unless substantiated on the ground. Substantiation of this information and gathering of significant amounts of new information was facilitated during a visit to Grand Cayman by the author in mid-October 2004. Throughout this project, and especially during that visit, I have been assisted by a number of individuals and organisations, many of whom are mentioned in the text of this report. A full list of acknowledgements is provided in the project summary report.

This report contains four further chapters. Chapter 2 describes in full the collection of data for the comprehensive analysis of hazardous phenomena. Chapter 3 presents the methodology for the analysis and the results. Chapter 4 provides a commentary on the results and a comparison with both short term forecasts on the basis of which emergency actions were taken and long term probabilistic hazard models on which long term planning decisions have been made. Chapter 5 provides a discussion of the area of the project covered by this report and a series of recommendations for action related specifically to more effective data gathering and hazards modelling.

This report has been written in such a way as to either explain or not use scientific jargon unless absolutely necessary. As such, it is hoped that it will be accessible to all readers, although an interest in tropical cyclones and their effects will be beneficial. It should be appreciated that analysis of data from Ivan is still ongoing in the scientific community, and some new data may become available over the next few months to years. Although such data is unlikely to change the basic story, this report cannot be regarded as definitive. It also should be noted that collection of detailed elevation data for Grand Cayman, such as could be used to accurately model the storm surge flooding, was ongoing at the time that this report was being prepared, and the results of that undertaking were not available in time to use them in this study.

The organisation mandated to forecast and analyse tropical cyclones in the Atlantic Basin is the National Hurricane Center (NHC, a division of the US Department of Commerce, National Oceanographic and Atmospheric Administration (NOAA), National Weather Service (NWS), Tropical Prediction Center (TPC)). NHC has released a post-storm summary analysis for Ivan and the research community most closely associated with the Hurricane Center (the Hurricane Research Division (HRD) of NOAA's Atlantic Oceanographic and Meteorological Laboratory (AOML)) will also likely release various scientific papers relating to Ivan. However, given the historically high activity during 2004 and especially the record 4 landfalling hurricanes in the US, it is unlikely that US researchers will take a more detailed look at Ivan during its passage past Grand Cayman than is presented here.

Clicking on any figure in this document will open a full resolution version of that figure, and clicking on blue-coloured hyperlinks will open referenced animations.

Times in this report are either in Coordinated Universal Time (UTC, equivalent to Greenwich Mean Time, given in 24-hour format *hhmm*), or in local time (for the period in question, 5 hours behind GMT/UTC, given in 12-hour format *hh.mm am/pm*).

Wind speeds are quoted as sustained 1-minute average at 10m height above open water (the standard NHC measurement). Gusts, where quoted are 3-second averages. Where other wind speed measurements are used, an explanation is provided in the text.

Distances and wind speeds are generally given in nautical miles (nm) and knots (kt) respectively; conversions are provided to miles and miles per hour (mph) in brackets. Small distance units (for flooding height etc) are given either in feet (ft) or metres (m). Rainfall is given in either inches or millimetres (mm). Where conversions are not provided in the text, the following factors can be used:

1 metre = 3.28 feet
1 foot = 0.305 metres
1 inch = 25.4 mm
1 mm = 0.0394 inches

1 nautical mile = 1.15 statute miles
1 statute mile = 0.869 nautical miles

1 knot = 1.15 mph = 0.514 metres/second
1 mph = 0.869 knots = 0.447 metres/second
1 metre/second = 2.24 mph = 1.94 knots

This page intentionally left blank

2 METEOROLOGICAL DATA GATHERING

Hurricane Ivan came closest to Grand Cayman between 1400 and 1600 UTC (between 9 and 11 am local time) on Sunday 12 September. The analysis of meteorological conditions concentrates on the period between 1200 and 2100 UTC, although sufficient information has been collected from both earlier and later in order to accurately define the time of onset of tropical storm and hurricane conditions on the island.

Meteorological information (which in this case includes storm surge and wave height information which would more accurately be termed oceanographic data) falls into two main classes; remotely sensed data and directly measured data. The former includes data from satellites and aircraft (as well as dropsondes released from aircraft) and the latter includes measurements made on the ground either during or after the storm's passage.

Wind data are relatively abundant from remotely sensed means, but are very limited from direct measurements. By contrast, sea condition data are not available from remote sensing but can be reconstructed to some extent from data collected on the ground after the storm. Rainfall data are available from remote sensing tools but are rare and generally rather inaccurate when collected on the ground.

The following two sections describe the main sources of data used in this study. Almost all of the raw data is in the public domain, although some is not readily accessible. All of the raw data is utilised in some form by the National Hurricane Center in its real-time analysis; however, a number of the satellite imagery processing algorithms utilised in this study are research tools not yet used during operational forecasting by the NHC. The availability of this new information has enabled a revision and improvement in the understanding of Ivan's destructive elements over that which could be garnered from the official NHC dataset.

The final section of this chapter discusses some 'missing' data as well as data which should continue to be collected in Grand Cayman in order to better quantify certain elements of the meteorological conditions.

2.1 Remotely-sensed data

Most data for tropical cyclones are collected remotely, either via satellite sensors or directly and indirectly via reconnaissance aircraft. All satellite data require interpretation in order to convert the raw visible, infra-red or microwave imagery into a credible meteorological model. Some aircraft data is also in the microwave field, but most is directly collected either via instruments on the aircraft itself or via instruments housed in dropwindsondes.

For almost all remotely sensed data, the state of hazardous phenomena at the surface (*e.g.* wind speed, surge height, wave height and rainfall) is at best a reasonable extrapolation and at worst a wild guess. Differentiating between good and bad data can be difficult, especially given the wide variety of data being collected and the rapidly developing techniques used to interpret the data.

The following data sets have been used to analyse the structure of Hurricane Ivan during its passage past Grand Cayman. As part of this project, almost all of this data has been geolocated and converted to a GIS-friendly format, imagery as geotiff format and data as shapefile format. Some data is also visualised via animated gif files. All of the data used in this analysis is provided on the accompanying CD-ROM.

2.1.1 Visible and infra-red (IR) satellite imagery from NOAA's geostationary GOES-12 satellite, collected at least every 30 minutes. Visible data is presented in black & white, IR data is colourised to show cloud top temperature. The IR colour scale goes from blue through green and red to yellow as temperature decreases and cloud top height increases, as shown in Figure 2.1.

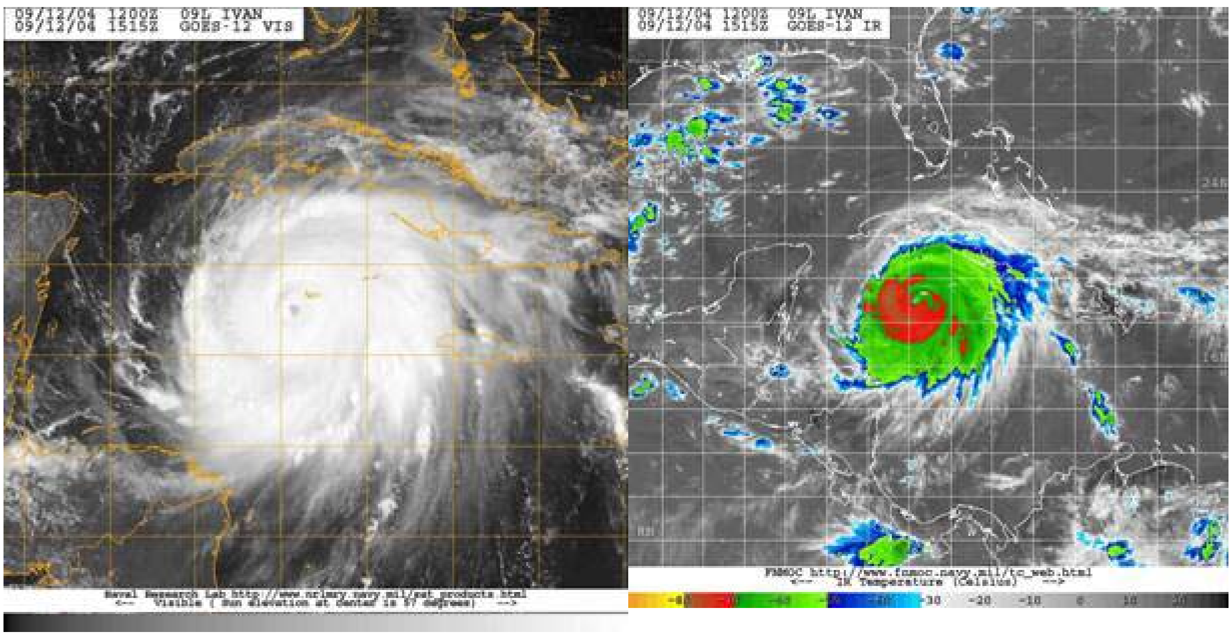

Figure 2.1 GOES12 visible (left) and infra-red (right) imagery of Hurricane Ivan for 1515 UTC (10:15am local) on 12 September 2004.

2.1.2 Microwave data (85 or 89GHz) from seven low-Earth orbiting satellite sensors; the Special Sensor Microwave/Imager (SSM/I) on DoD's Defense Meteorological Satellites Program (DMSP) -13, -14 & -15 satellites; the TRMM Microwave Imager (TMI) on the NASA/JAXA Tropical Rainfall Measuring Mission; the Advanced Microwave Scanning Radiometer for EOS (AMSR-E) on NASA's Aqua satellite; and the Advanced Microwave Sounding Unit-B (AMSU-B) on NOAA's -15 and -16 satellites. Coverage is uneven and relatively widely spaced compared to GOES coverage, averaging once every few hours for the Atlantic Basin (see example in Figure 2.2). A visualisation algorithm which combines and morphs the first five of the microwave sources listed above into a single pseudo-image every 15 minutes has been developed by scientists at the Cooperative Institute for Meteorological Satellite Studies (CIMSS) at the University of Wisconsin - Madison, creating an excellent research tool (Figure 2.2). Microwave imagery has the advantage of seeing through cloud tops, and essentially images hydrometeors (defined as any condensed form of water, larger than a single water molecule, that is falling or suspended in the atmosphere) in the cyclone. It is thus a very effective tool for imaging the eyewall and outer rain bands of a hurricane. The author gratefully acknowledges the MIMI team at CIMSS, particularly Chris Velden and Tony Wimmers.

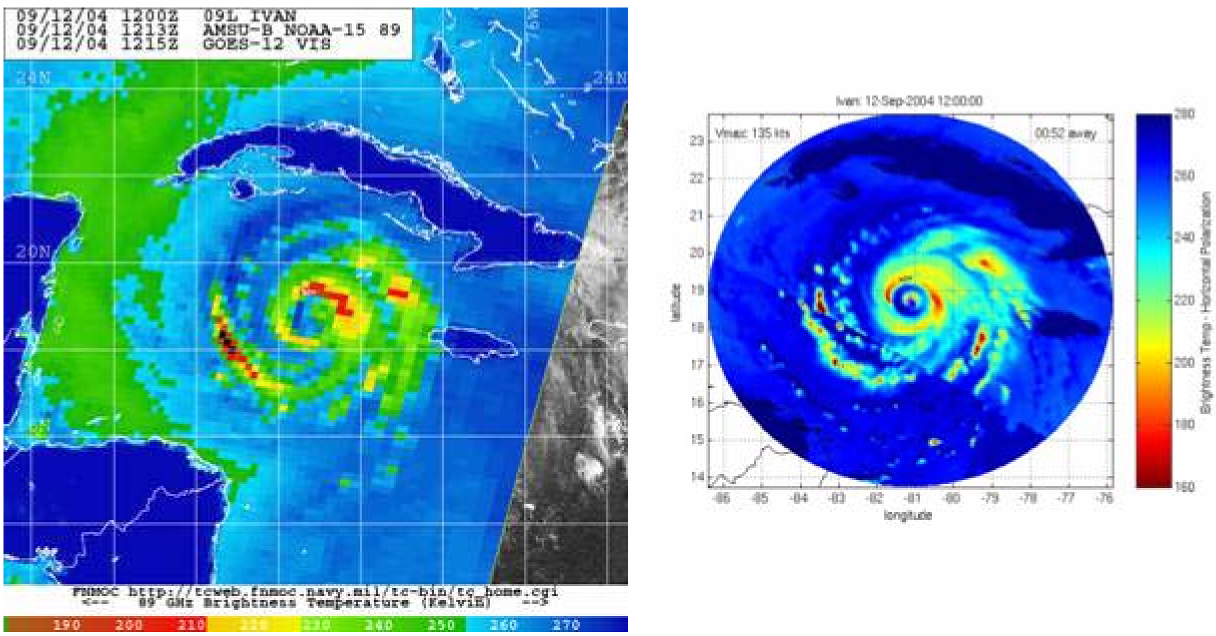

Figure 2.2 AMSU-B image from NOAA-15 at 1213 UTC (7:13am local) on 12 September (left) and the 1200 UTC (7:00am local) frame from the CIMSS morphing algorithm output movie for 12 September.

2.1.3 Output from the H*WIND algorithm developed by scientists at the Hurricane Research Division of NOAA's Atlantic Oceanographic and Meteorological Laboratory. H*WIND produces a wind field map (Figure 2.3) every 6 hours (or more frequently if necessary) which utilises data from stepped frequency microwave radiometer measurements of the sea surface from airborne reconnaissance flights. These measurements have been calibrated during the 2004 hurricane season by available GPS dropwindsonde data. The author particularly acknowledges the research undertaken by Mark Powell, HRD-AOML, who has pioneered wind field modelling for Atlantic tropical cyclones and provided valuable guidance during this project.

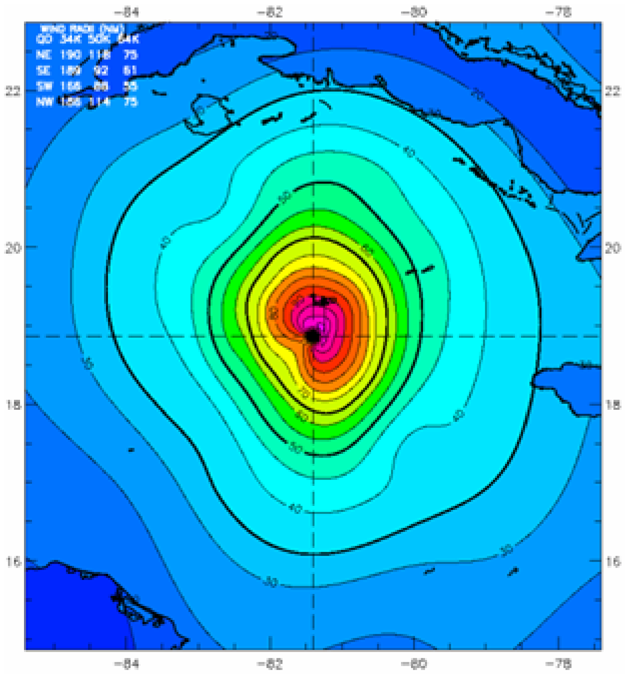

Figure 2.3 H*WIND output for Hurricane Ivan at 1330 UTC (8:30am local) on 12 September.

2.1.4 Flight level and GPS dropwindsonde data from NOAA and Air Force Reserve Hurricane Hunter aircraft flying reconnaissance missions. Four sets of recon data have been utilised in particular; vortex messages, which accurately locate the central point of the storm (URNT12); eyewall dropwindsonde data, which aim to pierce the strongest winds in the eyewall at the surface (URNT13); flight level winds recorded every 30 seconds during eye penetrations by the NOAA aircraft (URNT40) and flight level winds recorded every 15nm by all aircraft on vortex runs (URNT14). It should be noted that flight level winds are actually measured as a 10 second average, and dropwindsonde are measured as (effectively) a 5 second average. In both cases, because the measuring device is constantly moving through the area of peak wind, the 10 or 5 sec average is established as being representative of a 1 minute average measured at a fixed location. For the purposes of this analysis, aircraft reconnaissance data have been incorporated into a GIS shapefile format, with data points colour-coded for wind speed and shape-coded for data source. An example of GIS output showing reconnaissance data is provided as Figure 2.4. The author gratefully acknowledges the assistance of Mike Black, HRD-AOML, in finding, decoding and interpreting dropwindsonde data.

2.1.5 National Hurricane Center official position and intensity information (Figure 2.4), issued every 3 hours, and gross wind field shape information, issued every 6 hours. Both of these data sets are the result of combination and interpretation of most of the data listed above, as well as radar imagery from reconnaissance aircraft and land sites (if available). The real-time NHC position/intensity product is reviewed in post-season analysis, and a 'best track' is issued which serves as the definitive official record of the storm. In the case of Ivan, the best track was issued by NHC on 16 December 2004.

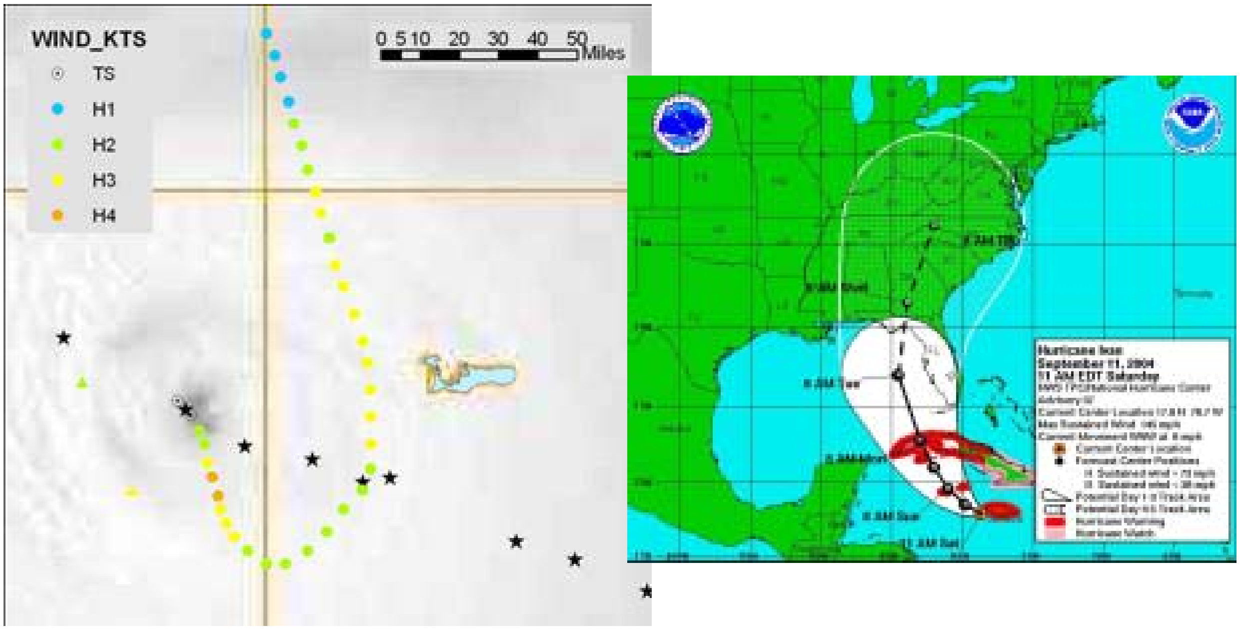

Figure 2.4 GIS output of reconnaissance data for Hurricane Ivan (left) and visualisation of NHC forecast track and intensity and current wind field (above).

2.1.6 Global meteorological models, which are increasingly used to investigate the gross characteristics of hurricanes, and provide a low resolution but potentially useful constraint on wind field models. During this exercise, two major public-domain models were run for Ivan's passage past Grand Cayman; the Weather Research and Forecast (WRF) model and the MM5 model, both developed under the auspices of the US University Consortium for Atmospheric Research (UCAR). The MM5 model has too low a resolution (36km) to be useful in this case for the hurricane wind field. The WRF model has 12km and some 4km resolution data but even here, the resolution is not sufficient to adequately model the innermost (and highest) winds in the hurricane. Figure 2.5 shows examples of the model outputs. The author gratefully acknowledges the assistance of George Waldenburger and Robert Fovell, Department of Atmospheric and Oceanic Sciences at the University of California, Los Angeles, for assistance in running these models.

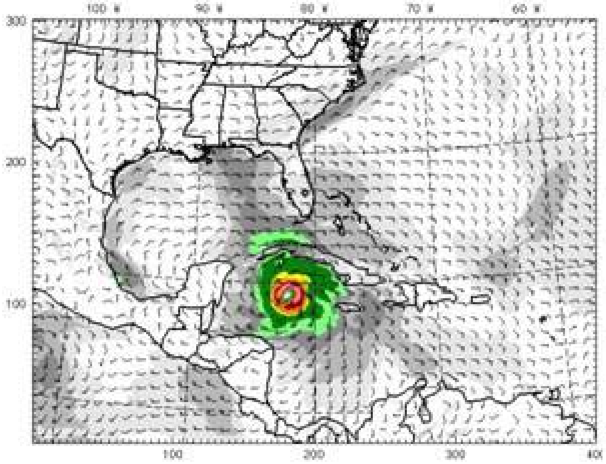

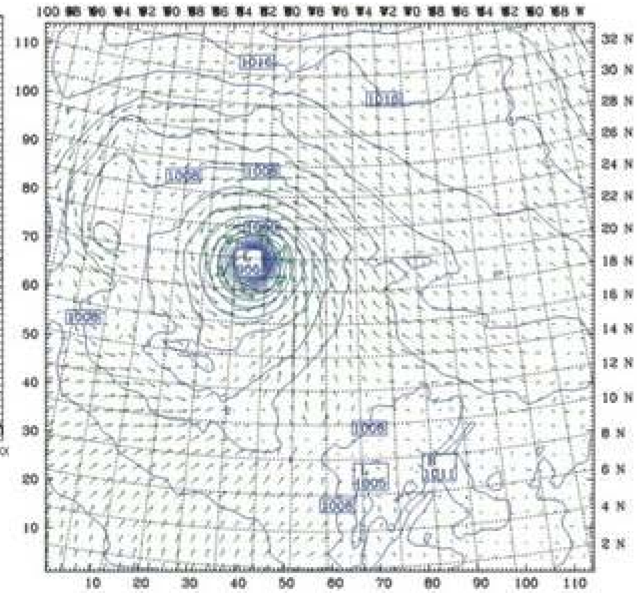

Figure 2.5 WRF (above) and MM5 (right) model output for Hurricane Ivan at 1800UTC on 12 September.

2.2 Directly measured data

Directly measured data fall into two distinct categories. The first is quantitative data collected during the passage of the storm, either by meteorological instruments on the ground (for wind speed and rainfall) or by oceanographic instruments on piers or buoys (for storm surge and wave heights). The second is quantitative and qualitative data collected either from physical evidence (tide marks, damage *etc*.) or from personal recollection (*e.g*. timing of events, direction of flood movement etc), both collected during a post-hoc survey.

The first of the above groups of potential data is alarmingly small. Despite the presence of a number of meteorological stations on the island including those run by the National Weather Service of the Cayman Island Government, by ham radio operators (furnished by NOAA) and by amateur meteorologists, only one anemometer recorded anything approaching a maximum wind speed and only one rain gauge recorded a reasonable rainfall measurement. The anemometer in question was severely compromised during the storm (Figure 2.6), and stopped recording before the peak winds were encountered. There were no reliable measurements of the minimum pressure encountered. Some early wind and pressure measurements have been used to provide some validation of remotely sensed information.

There were no tide gauges or other oceanographic instruments operating in Grand Cayman during the passage of Ivan, and there are no moored or drifting buoys in the area around the island. Therefore there were no directly measured wave or storm surge heights for Ivan in the vicinity of Grand Cayman.

Figure 2.6 Location of the only working anemometer during Ivan, in the home of Mike Whiteman in West Bay. Above is before, below is after.

Information gathered during the post-hoc survey in mid-October 2004 provides an invaluable supplementary data set. It is hoped that this data set will continue to be added to as more information is collected by the various agencies in Cayman undertaking post-impact studies (see following section for more details).

The post-hoc data set comprises:

- Flood water levels measured from water marks on buildings and associated personal recollections

- Flood water timing and direction of flow, both from personal recollections

- Wave height estimation from height of wave damage levels and from personal recollections

- Local variations in peak wind speed and direction from vegetation and building damage

The post-hoc survey undertaken by the author was greatly facilitated through the guidance of Mike Whiteman, a government surveyor and true man of science. Mike's knowledge of the island, photo-documentation in the immediate aftermath of Ivan, dedication to collecting data during the peak of the storm and ability to find important people are all gratefully acknowledged.

2.3 'Missing' data and further data collection and analysis

Several data sets utilised during this project are either incomplete or are subject to revision. None are vital to the modelling of the hazardous impacts of Ivan in Grand Cayman, although better validation of the results may be possible if some or all of these data become available. The key missing data or useful additions to data sets are as follows:

- Some data from the Air Force Reserve Hurricane Hunter flights are not publicly available; specifically, the SXXX50 data (equivalent to the URNT40 messages from the NOAA aircraft) have not been located in the public domain, despite several requests to NOAA

- Due to time constraints, a complete analysis of all dropwindsonde data has not been undertaken – instead, decoding and analysis of key dropwindsonde datasets has been undertaken. Mike Black at HRD-AOML will likely undertake a more rigorous analysis of dropwindsonde data for Ivan sometime in the future

- Ground level wind data may have been collected at two sites in Grand Cayman during Ivan, but as yet, these data have not been made available

- Additional data concerning personal recollections and physical evidence for wind, surge and wave action during Ivan continues to be collected on Grand Cayman, primarily by the Lands and Survey Department but also by the Department of Environment. Both of these agencies were briefed on the type of data to be collected

- Detailed topographic data and before and after photographic images are both being processed in the Lands and Survey Department but were not available at the time of writing this report. In the absence of good topographic control, a surge flooding map could not be drawn, and surge and wave heights are only estimates. The high resolution photographic images will be useful in observing local variations in winds and water damage which may be due to primary meteorological factors or to differences in building vulnerability

3 SUMMARY AND INTERPRETATION OF THE METEOROLOGICAL DATA

The nature of the meteorological data available for this investigation has been described in the previous chapter. Interpretation of these disparate sets of data is made especially difficult in this case due to the lack of reliable data from the ground, especially in terms of wind speed. This lack of hard data from 'ground zero' of a severe hurricane impact in the Caribbean is a frustrating situation repeated every year across the Caribbean, and is the subject of one of the key recommendations of this study, namely the construction and upkeep of a network of meteorological instrumentation to consistently and reliably record the nature of the hazards associated with tropical cyclones in the region.

This chapter discusses the reliability of the available data and presents a summary of both the general meteorological conditions encountered and the best quantitative estimate of the level of hazardous phenomena encountered on Grand Cayman. The results of the accompanying engineering study of damage to infrastructure in Grand Cayman provides some feedback to the credibility of the meteorological model presented here. However, post-hoc analysis of building damage as has been undertaken for this project does not provide sufficiently robust data, in terms of the quantitative level of hazardous phenomena encountered, to influence the meteorological model.

3.1 Reliability of data

Assessing the reliability of the data described in the previous chapter is critical to formulating a credible model of the hazardous phenomena encountered during the passage of Hurricane Ivan past Grand Cayman. This section briefly reviews the reliability of the actual data and the robustness of the interpretations used in this assessment.

The single actual measurement of peak wind speed during Ivan was that made by the anemometer of Mike Whiteman in West Bay. The reliability of this information is difficult to assess given that the anemometer mast had been compromised (bent to about 40 degrees downwind) several hours prior to the peak reading being made. Even without that compromise, the accuracy of the anemometer in high winds is unknown. Experience of similar instruments in other hurricanes suggest that they generally over estimate wind speeds, sometimes very significantly (Powell *et al*., 1996). A further difficulty with these data is that the wind speed wasn't being logged automatically; Mr Whiteman and his wife monitored the digital readout for 1 minute every 15-30 minutes and mutually decided on an average and peak wind speed for each 1-minute period. Experience from other situations where similar procedures have been followed suggests that, even with the best will in the world, an overestimate of the average will likely occur. However, the maximum gust measurement is likely to be sound.

Whiteman's 'peak' wind speed almost certainly was not a measurement at the time of peak winds in the West Bay area. The anemometer stopped registering meaningful data soon after the highest wind measurement at 10am local time, but Whiteman's roof was further compromised in the following hour. The meteorological model constructed must take account both of the potential errors in the Whiteman data and of the fact that the 'banner' peak recorded wind speed was probably not a true representation of the real peak.

Table 3.1 summarises the likely errors in the Whiteman anemometer data.

Cause of error	Likely max error (+ve is overestimate)
Bent anemometer mast	Unknown, intuitively –10%
Anemometer measurement error in high wind	Untested, probably +20%
Data recording error	Probably +5%, none for gusts
Height and exposure	Minor compared to other errors

Table 3.1 Likely errors in the Whiteman anemometer data

Other data from the ground, as described in the previous chapter, comprises rainfall data, storm surge height and wave height. The rainfall data collected at the airport almost certainly represents a minimum, as strong winds tend to drive rain across a rain gauge, thus lowering the amount falling into the gauge. Storm surge and wave height estimates come either from personal accounts or from measurements of impact and tide marks on buildings. All of these data sources are inherently inaccurate, but with sufficient care in collection and sufficient sampling density, such inaccuracies can be reduced to reasonable levels.

The remotely sensed data used in this study all have excellent quality control so that the raw data can be regarded as error-free. However, conversion of raw data into a useable 'product' with which to estimate surface parameters is prone to error, and is also partially subjective. In this exercise, the author has attempted to revise the NHC real-time analysis of location, intensity and wind field in the light of data not available to NHC forecasters at the time. Such a process should not, in itself, introduce errors; instead, it can be regarded as a modest re-interpretation in the light of strong quantitative and other qualitative data. As is discussed in the next section, the key elements of reconnaissance flights and the morphed microwave data highlight an important eye-wall replacement cycle between 1200 and 2100 UTC on 12 September which, although briefly mentioned in the NHC discussion product, is not represented in the real-time NHC output.

The most significant error introduced in converting remotely sensed data to surface level conditions is the projection of flight level wind speed to surface level wind speed (by which we mean the wind speed at 10m above ground level over open water). The increasing database of dropwindsonde information is assisting in making this conversion more rigorous; however, there are still significant variations in the conversion factor between and even within storms.

The rule-of-thumb conversion factor from flight level (~10,000ft) to surface winds is 0.9 for the eyewall and 0.8 for the outer parts of the storm. Further to this, dropwindsonde peak surface winds in the eyewall are typically ~80 % of the peak flight level wind on a particular leg. Due to the outward radial tilt of the maximum wind with height in the eyewall, it is possible to get significantly higher winds at the surface than at flight level for an eyewall dropwindsonde.

Within this project, a small number of dropwindsonde profiles have been analysed for Hurricane Ivan while in the vicinity of Grand Cayman; these suggest that these rules-of-thumb are reasonable.

In conclusion, the conversion of various remotely sensed data to surface level winds and the non-definitive nature of the entire data set without a well-calibrated ground control point lead to a likely final wind speed error estimate of 5 to 10%. This error is consistent with NHC estimates, for example the recent upgrade of Hurricane Andrew (Landsea *et al*., 2004).

3.2 Summary of Ivan's passage past Grand Cayman

This section summarises the status of Hurricane Ivan during its passage past Grand Cayman. It is based on analysis of all of the information sources summarised in the previous chapter. This section includes a large number of diagrams to illustrate relevant parts of the meteorological story. Although Grand Cayman is a small island, there were considerable variations in the meteorological conditions across the island; these are partially illustrated by the use of three key locations in the analysis, West Bay, George Town and East End. Other local variations are highlighted in the text.

The accompanying CD-ROM contains a comprehensive database, much of it in GIS format, so that interested parties can reproduce and illustrate the passage of Ivan for themselves. Within this report, key images are embedded in the report and hyperlinks point to associated data, either in the form of images or movies.

3.2.1 General overview of Hurricane Ivan

Hurricane Ivan was a classic Cape Verde cyclone, particularly notable for its southerly track and its persistent high intensity. Figure 3.1 shows the track, with colour coding showing the intensity of the hurricane (measured by the maximum estimated wind speed within the storm). A hotlink from Figure 3.1 plays an animation of GOES-IR imagery for Ivan's track past the Cayman Islands. Ivan began as a large, though poorly formed tropical wave off the west African coast on 31 August, attaining Tropical Depression status on 2 September and Tropical Storm status early on 3 September. Despite maintaining a westerly course south of 10°N (the accepted southern limit of the hurricane strengthening zone), Ivan continued to strengthen, achieving Hurricane status at 0600 UTC on 5 September and becoming the most southerly severe hurricane on record during a dramatic intensification phase over the next 24 hours.

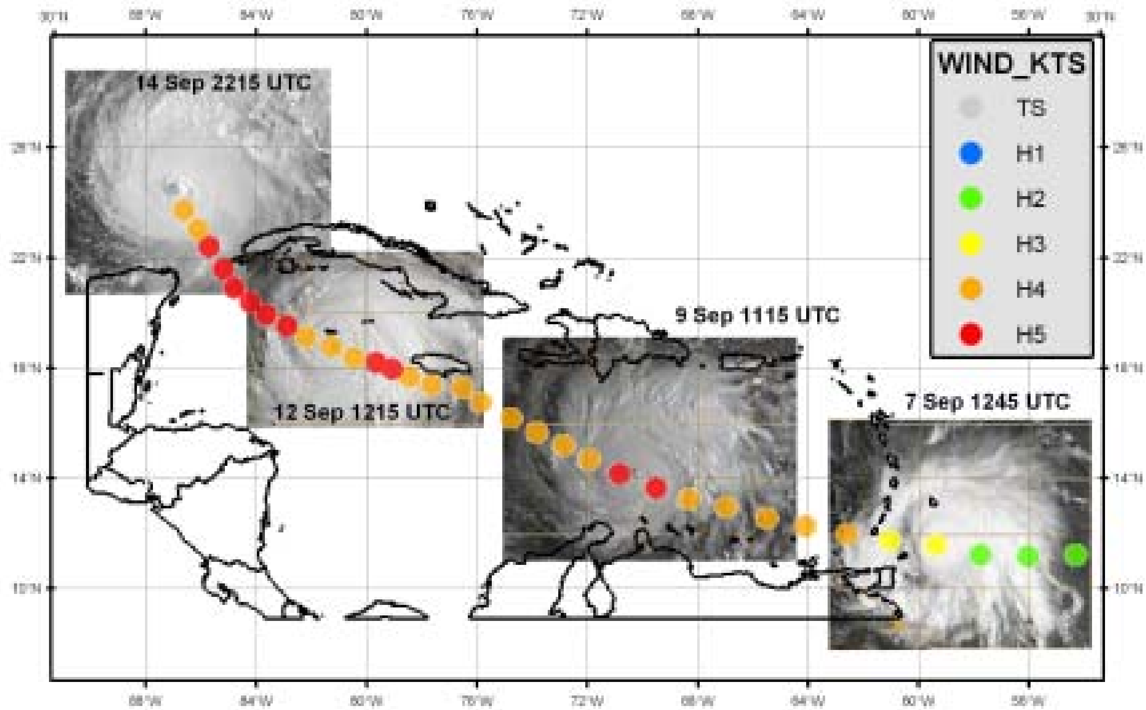

Figure 3.1 Full official track of Hurricane Ivan from passing Barbados on 6 September to its exit from the Caribbean Sea through the Yucatan Passage on 14 September. Selected GOES-12 satellite images illustrate the state of the storm. Note that the hurricane intensity key colours are the same for all figures in this report. Click here for an animated series of GOES imagery for Ivan.

After a brief de-intensification, Ivan regained severe hurricane status (Category 3, winds greater than 96 kt, 110 mph) as it passed south of Barbados into the Caribbean Sea around midday (UTC) on 7 September. According to the NHC post-storm best track data, Ivan attained Category 4 status as it passed Grenada late on 7 January (Figure 3.2) and was at Cat 4 or Cat 5 (winds greater than 130 mph) throughout its passage across the Caribbean Sea, exiting into the Gulf of Mexico on 14 September. While crossing the Caribbean Sea (Figure 3.3), Ivan achieved Category 5 status (winds greater than 135 kt, 155 mph) on three different occasions, the final two being immediately before and immediately after the 18 hours when the storm was closest to Grand Cayman.

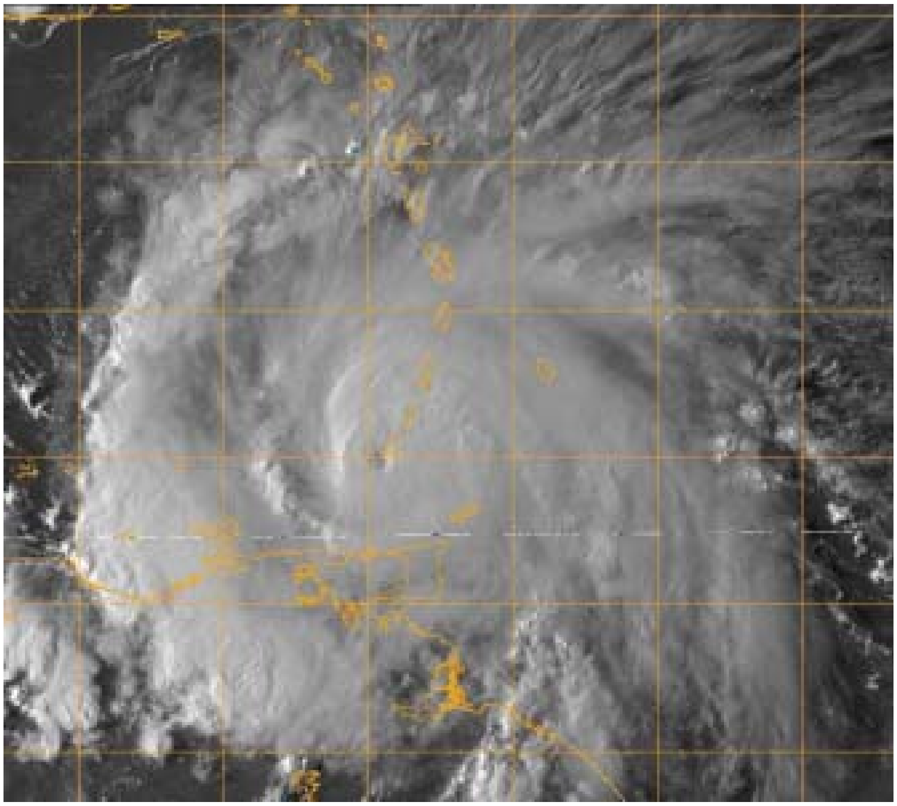

Figure 3.2 Hurricane Ivan crossing the southern tip of Grenada and entering the Caribbean Sea. GOES-12 visible image from 2045 UTC on 7 September 2004.

Figure 3.3 Hurricane Ivan passing Grand Cayman. Visible imagery from GOES-12, 1745 UTC on 12 September 2004. More imagery available on CD-ROM.

Ivan's passage through the Caribbean brought Hurricane strength winds (>74 mph) to Grenada (Category 3), Jamaica (Category 1-2) and Grand Cayman (Category 4) and Tropical Storm force winds (39-74 mph) to Barbados, St Vincent & the Grenadines, Tobago, Little Cayman and Cayman Brac. With these winds came a moderate storm surge and heavy waves, especially along Jamaica's south coast and in Grand Cayman. Ivan will be remembered for the devastation it brought to Grenada and Grand Cayman, for its southerly track and for its persistent status as a severe hurricane.

3.2.2 Characteristics of Ivan between 11 and 13 September

Ivan's passage past Grand Cayman occurred between 11 and 13 September, during which time it achieved its highest measured wind speed (flight level (10,000 ft) wind of 161 kt (185 mph) at 1917 UTC on 11 September) and its lowest pressure (910 mb extrapolated from flight level at 0005 UTC on 12 September). During this same period, Ivan underwent an eyewall replacement cycle which led to a lowering of peak wind speeds between 0600 UTC on 12 September and 0000 UTC on 13 September. This eyewall replacement cycle was the key element in controlling the wind speed encountered on Grand Cayman; it led to a decrease in the peak wind speed encountered on the island, but an increase in the duration of strong winds, especially after the storm had passed its closest approach.

The intensity of the storm and its position relative to Grand Cayman influenced not only the winds felt on the island, but also the nature of the wave and storm surge hazards. Early winds came out of the northeast and produced a high storm surge in North Sound; later winds from the southeast produced a second surge peak from South Sound and also heavy wave action along the South coast and along the south-facing coastal stretch of West Bay. Rainfall was sporadic but heavy and lasted well beyond the period of most intense wind.

Figure 3.4 summarises the windfield of Ivan for this period. It shows the previous and forecast future wind bands and the actual windfield at each 3-hourly forecast time from 1500 UTC on 10 September until 1200 UTC on 13 September. In addition to showing the scale of the wind field for Ivan, it also highlights the right-bias of the forecast, which is further discussed in the next chapter. This plot represents the real time NHC official output, which gave a position and intensity estimate every 3 hours and windfield dimensions (distance to 34, 50 and 64 kt winds in each quadrant) every 6 hours.

The official real time position and intensity estimates for Ivan on 12 & 13 September were changed a little by NHC in the post-season analysis; these changes comprised very minor shifts in the location of the centre of the storm at 0000 and 1800 UTC on 12 September, a reduction in the estimated intensity at 0600 UTC on 12 September (from 145 to 135 kt, a change which occurred in the real time estimate 3 hours later) and an increase in the intensity at 0000 UTC on 13 September (from 130 to 140 kt, a change which occurred in the real time estimate 3 hours later).

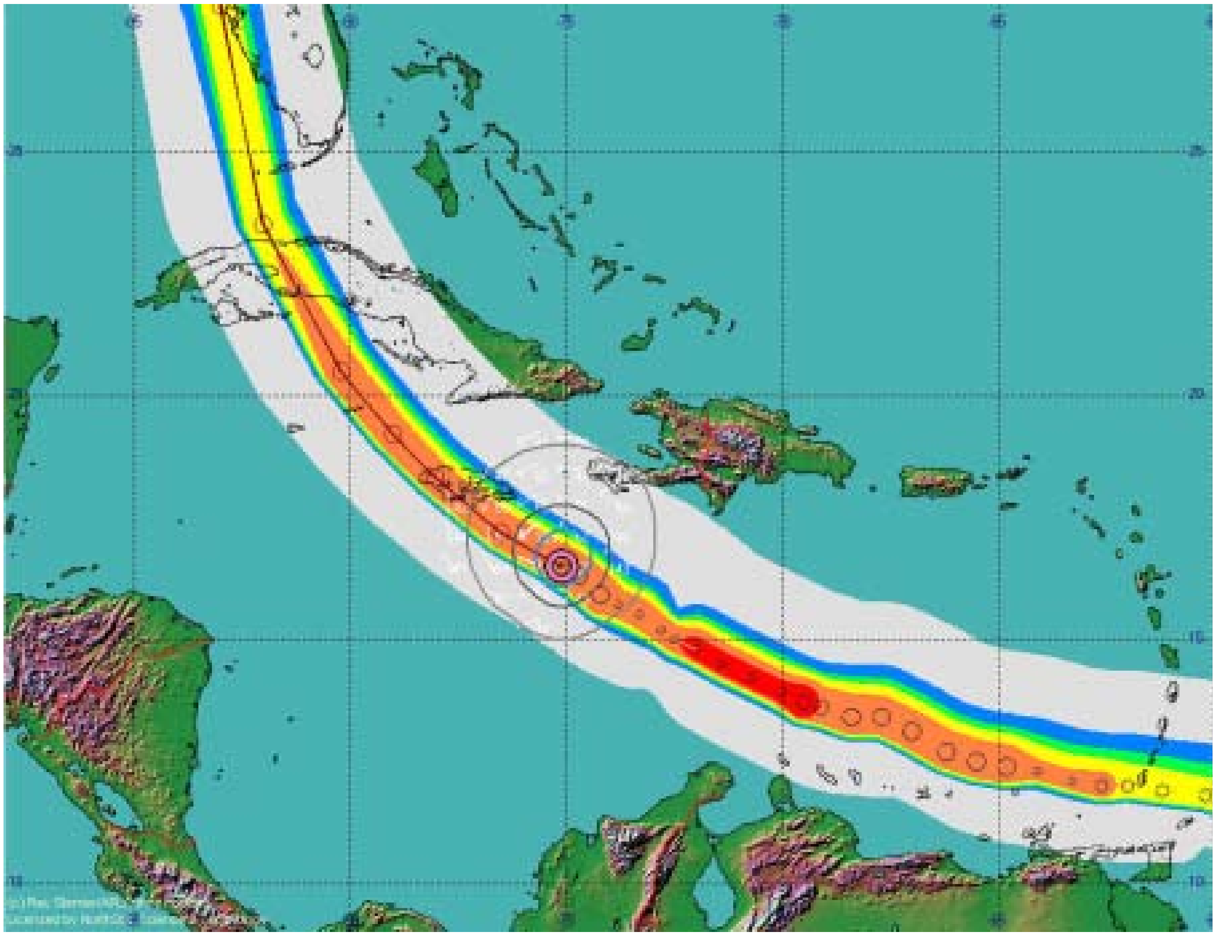

Figure 3.4 Windfield for Ivan during its passage past Jamaica and Grand Cayman, starting at 1500 UTC on 10 September. Click here to play the animation.

Some discrepancies between the official forecast and a near real time NHC product providing more detailed windfield analysis (known as H*WIND) acted as a starting point for the post storm analysis of windfield presented here. The changes made in the NHC 'best track' do not address these discrepancies. The relevant H*WIND outputs are shown in Figure 3.5. As can be seen, these outputs give estimated wind speeds on Grand Cayman considerably below those recorded by anemometer (even allowing for the likely overestimation in those anemometer records). Further evidence from airborne measurements and dropwindsondes support the notion that, in this case, the H*WIND analysis underestimates peak wind speeds in key areas.

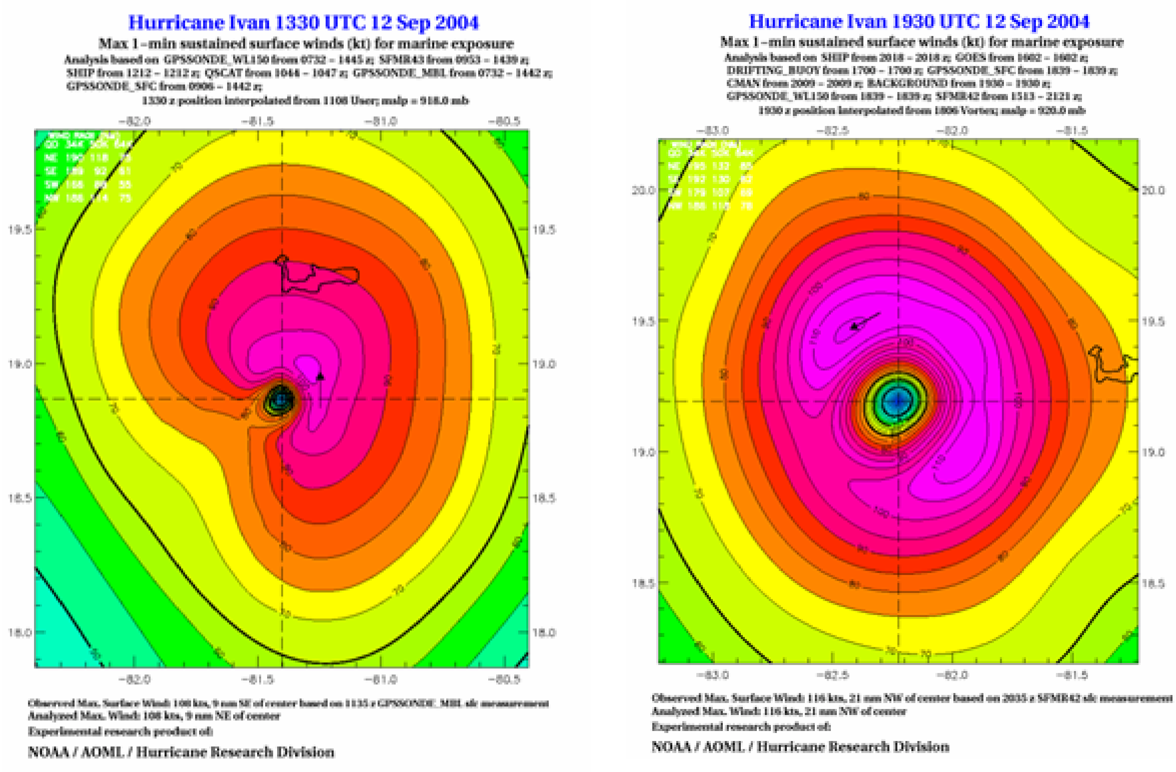

Figure 3.5 H*WIND analysis for Ivan at 1330 and 1930 UTC on 12 September. Although the likely peak in winds on Grand Cayman occurred midway between these times, the overall trend of these H*WIND analyses is to underestimate the wind speeds. Complete suite of H*WIND outputs for 11-13 September available on CD-ROM.

The key meteorological phenomenon causing most of the discrepancies is known as an eyewall replacement cycle. Such cycles occur in all powerful hurricanes and provide the mechanism for sustaining hurricanes at Category 4 or 5 for prolonged periods. The details of eyewall replacement will not be discussed here; instead, Figure 3.6 provides a superb illustration of a classic eyewall replacement cycle which just happened to occur as Ivan was passing Grand Cayman. The images and movie in Figure 3.6 are the product of the Morphed anImated Microwave Imagery (MIMI) research project at the University of Wisconsin – Madison, where a diverse set of microwave satellite images are merged together and animated into a succession of images at 15-minute intervals. Microwaves are particularly useful in hurricane research as they are able to see through the upper clouds into the heart of the hurricane, and image the eyewall of a storm particularly well.

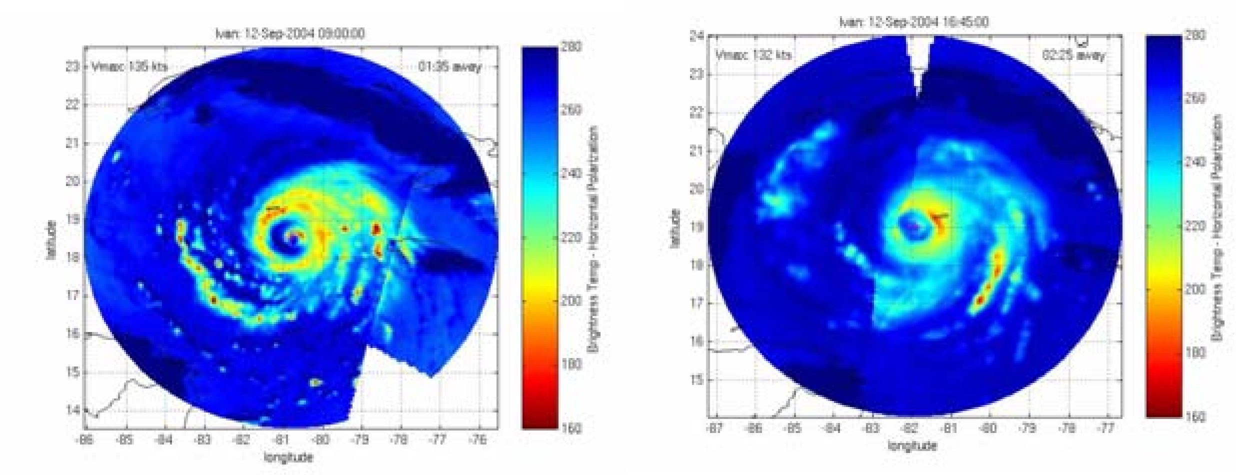

Figure 3.6 Morphed microwave imagery for 0900 (left) and 1645 UTC (right) on 12 September. Click here to play the animation, which covers the period 0700 UTC on 12 September to 0000 UTC on 13 September.

The 0900 MIMI image shows a small, tight eyewall to the SSE of Grand Cayman with highest winds in the northern half of the eyewall (red colours in a semicircle to the north of the centre). Over Grand Cayman itself is an intense rainband which is starting to form a closed circle. Ivan is waning in intensity at this point at 135 kt, having peaked a few hours earlier at 145 kt maximum wind. The waning is due to initiation of eyewall replacement, where peak winds are falling in the inner eyewall but rising in the intense rainband. Over the next 8 hours or so, the inner eyewall breaks down and the intense rainband develops into first an outer eyewall and then the main eyewall, as shown in the 1645 MIMI image. In this later image, it can be seen that Grand Cayman is within this outer eyewall as it becomes dominant, even after the centre of the storm has made its closest pass. The outer eyewall is intensifying as it clears Grand Cayman, reaching 140 kt a few hours later at 0000 UTC on 13 September. Another consequence of the eyewall replacement cycle was the slowing of forward speed of the hurricane, from about 11 kt early on 12 September to around 5 kt late on 12 September.

With this basic model as a foundation, the re-analysis presented here incorporates airborne and dropwindsonde data to act as control points on the windfield. Figure 3.7 shows two sets of key eyewall dropwindsonde profiles taken in locations close to Grand Cayman during the period of eyewall replacement. These two profile sets are chosen as representative of the vertical windfield distribution in the areas of peak winds at 1500 and 1945 respectively, and the conversion factor from flight level to ground level deduced from these profiles is used to convert the abundant flight level data in and around the eyewall for the respective time periods. It should be noted that the conversion factors are very close to those used in rule-of-thumb calculations by NHC.

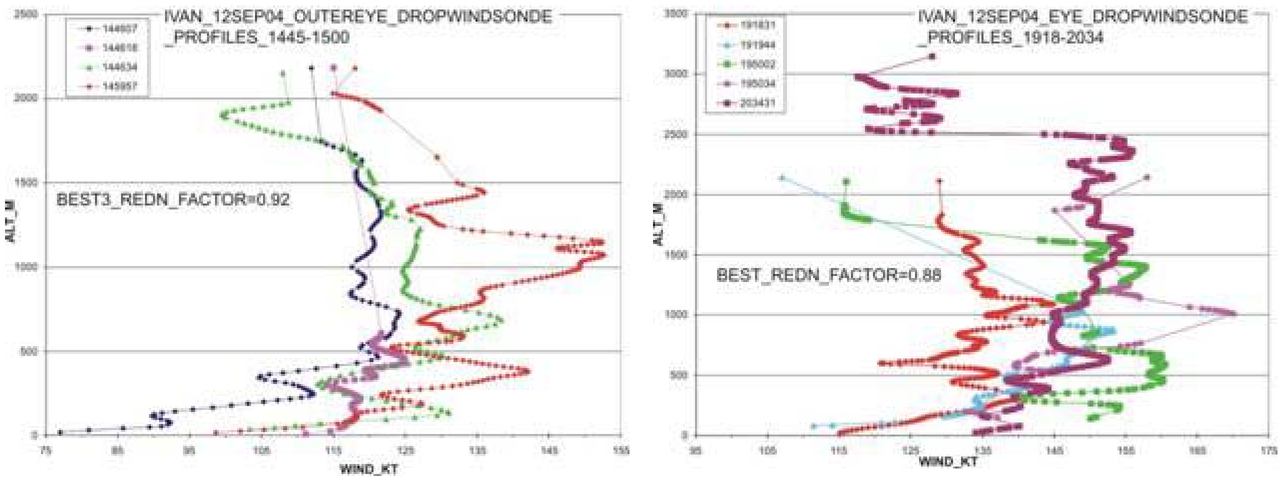

Figure 3.7 Representative eyewall dropwindsonde profiles for 1500 (left) and 1945 (right) UTC on 12 September.

Figures 3.8 to 3.15 show a succession of plots from ArcView GIS (ESRI software) at key intervals in the passage of Ivan past Grand Cayman. These plots show the development of the storm through snapshots incorporating all of the relevant data. The key for all plots is the same. Basic wind radii and airborne data points are colour coded to wind speed and the source of the wind radii is given. The background satellite image type and time is provided in the title. All wind speeds are in mph and all times are UTC. Circles on the plot represent flight level winds, triangles represent surface winds, either measured or converted from flight level. Key wind speed data are marked; these marked data points comprise all actual surface measurements and also the peak wind speed from each run of flight level data for each side of the storm.

In addition to affecting the ‘headline’ wind speed encountered on Grand Cayman, the location and intensity of the hurricane also affects the storm surge and wave action. Wind direction was especially important in controlling storm surge flooding and wave damage; the effective expansion and intensification of the eyewall after the storm had made its closest pass of Grand Cayman brought strong onshore winds around to the south coast of the island increasing storm surge flooding and causing extensive wave damage after the peak winds had passed. The actual status of wind, surge and wave hazards are described in the next section.

The evolution of the storm as it passed Cayman did not greatly affect the rainfall pattern; however, the slowdown in effective forward speed meant that the total rainfall was significantly higher than would be normal for a similar storm.

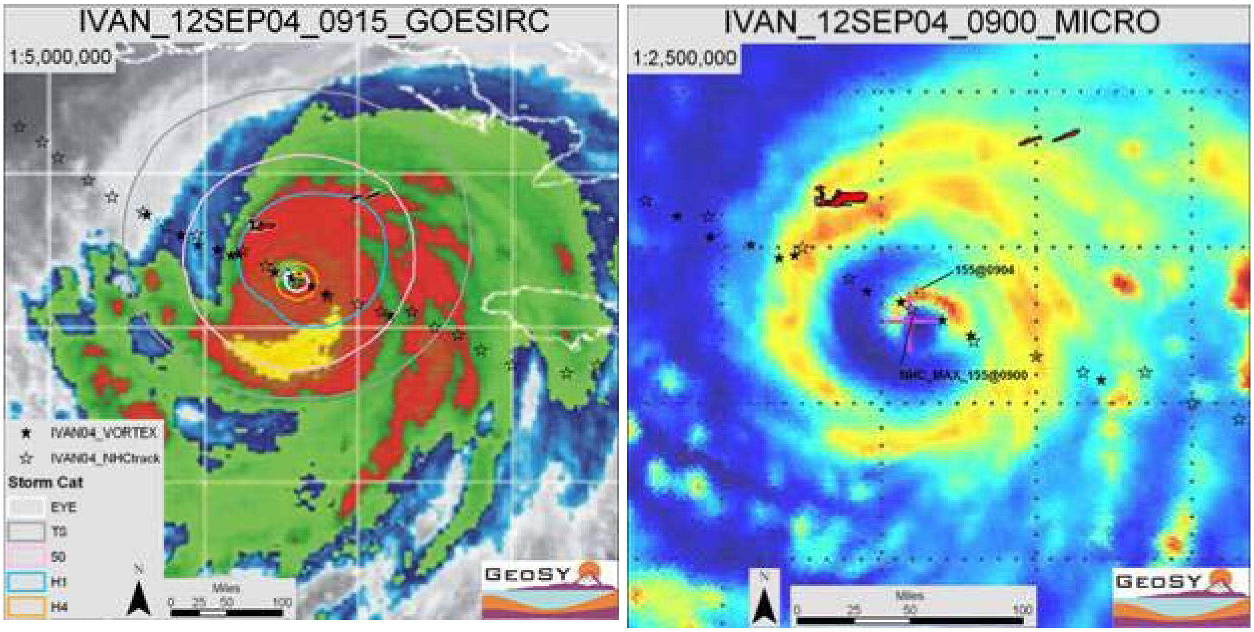

Figure 3.8 GOES infra-red (left) and morphed microwave (right) imagery for the period around 0900 UTC (4 am local time) on 12 September. Peak winds (155mph) are in the northern eyewall of a compact eye structure. Grand Cayman is beneath a broad, locally intense rain band, with hurricane force winds being felt over almost all of the island.

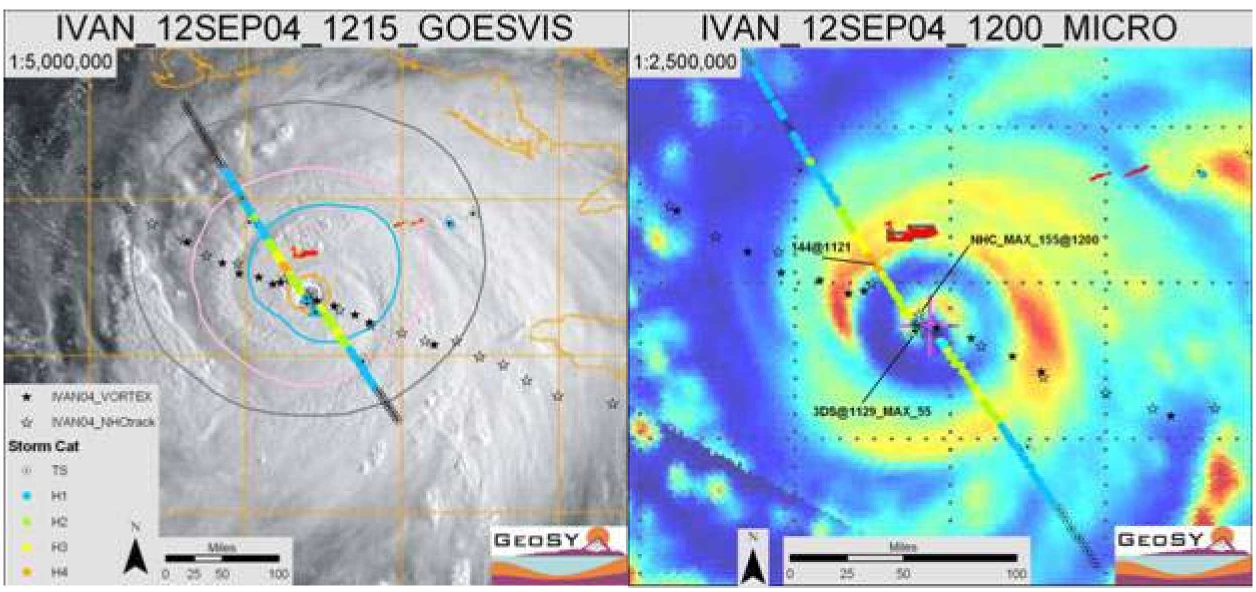

Figure 3.9 GOES visible (left) and morphed microwave (right) imagery for the period around 1200 UTC (7 am local time) on 12 September. The NHC interim intensity remained at 155mph, but airborne data show that the inner eyewall was rapidly collapsing and peak winds had probably switched to the outer eyewall. The peak flight level wind of 144 mph suggests that the NHC intensity may be an overestimate at this time.

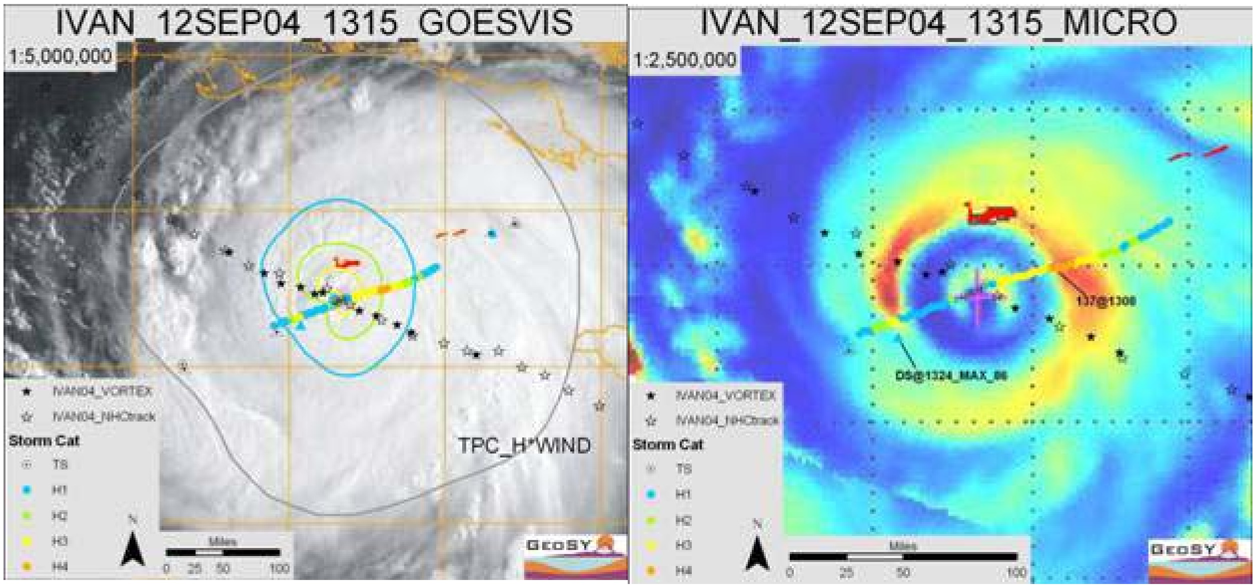

Figure 3.10 GOES visible (left) and morphed microwave (right) imagery for the period around 1315 UTC (8.15 am local time) on 12 September. The image at left shows the wind radii from the NHC H*WIND analysis for 1330 UTC. As is clear from the airborne data, supported by the microwave image, the H*WIND analysis does not successfully model the strengthening outer eyewall at this time.

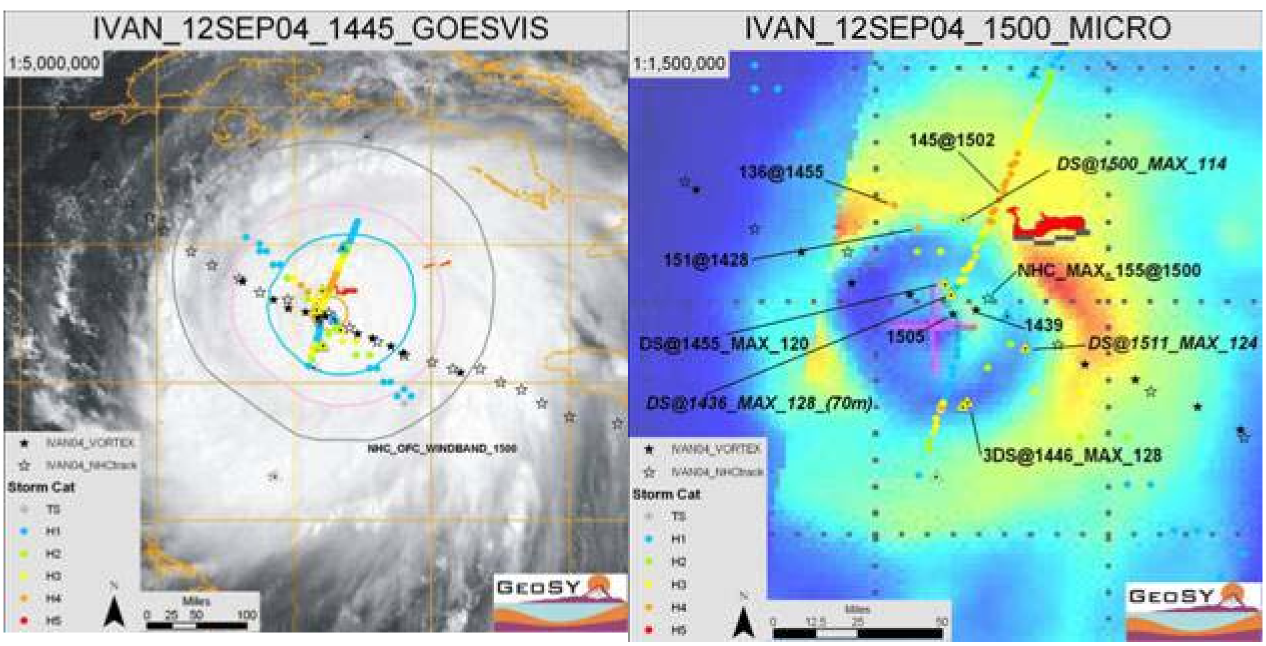

Figure 3.11 GOES visible (left) and morphed microwave (right) imagery for the period around 1500 UTC (10 am local time) on 12 September. The centre of the storm has just passed its closest approach to Grand Cayman, and strongest winds are in the northern outer eyewall close to the island.

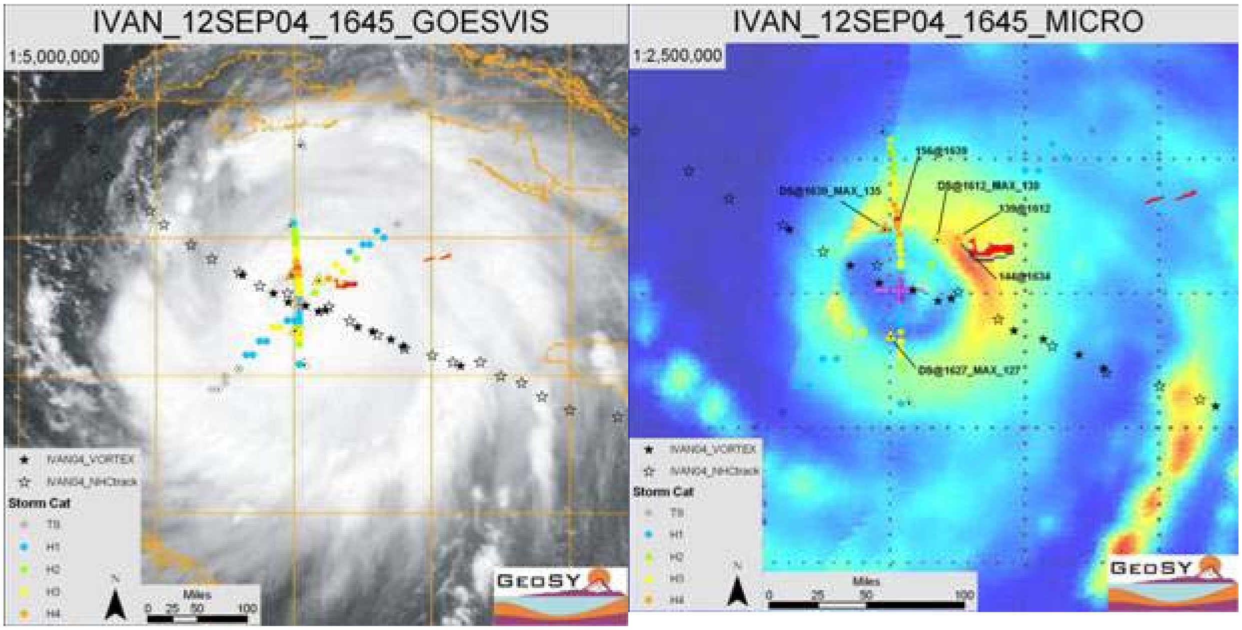

Figure 3.12 GOES visible (left) and morphed microwave (right) imagery for the period around 1645 UTC (11.45 am local time) on 12 September. The western part of Grand Cayman is just outside the northeastern segment of the eyewall, and peak winds just offshore to the west, as measured at flight level, have remained constant over the previous 2 hours.

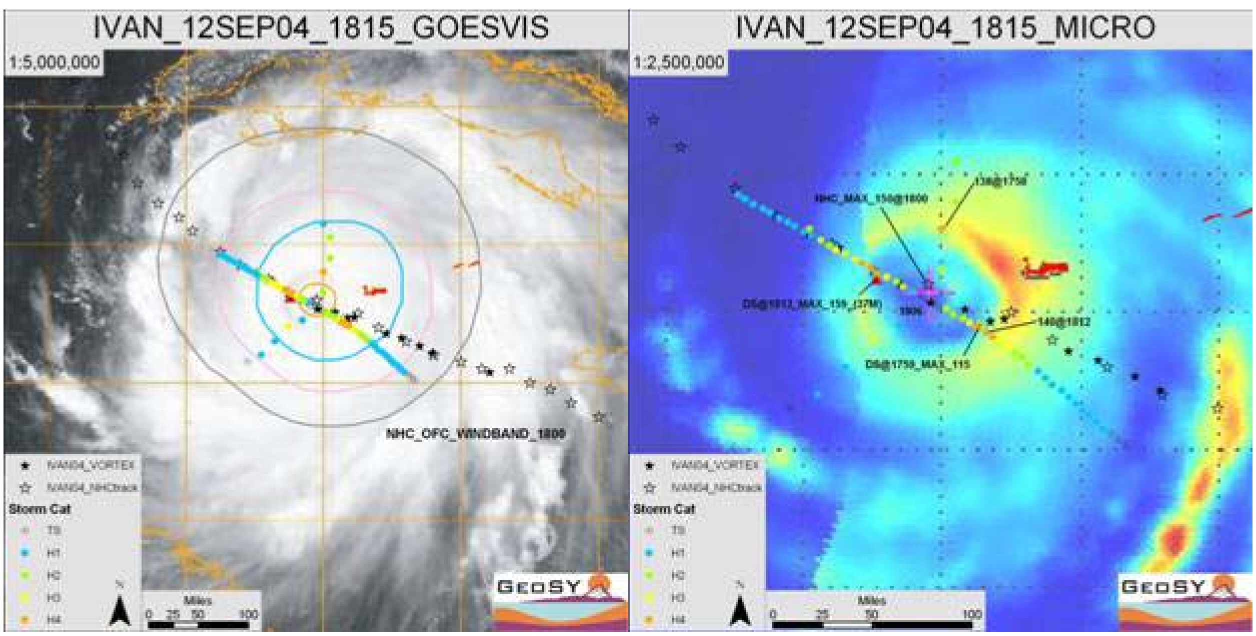

Figure 3.13 GOES visible (left) and morphed microwave (right) imagery for the period around 1815 UTC (1.15 pm local time) on 12 September. The NHC official windfield shows Grand Cayman near to the edge of the hurricane force winds at this time; however, the microwave imagery, supported by airborne data, shows that the western part of Grand Cayman is still close to the area of highest intensity.

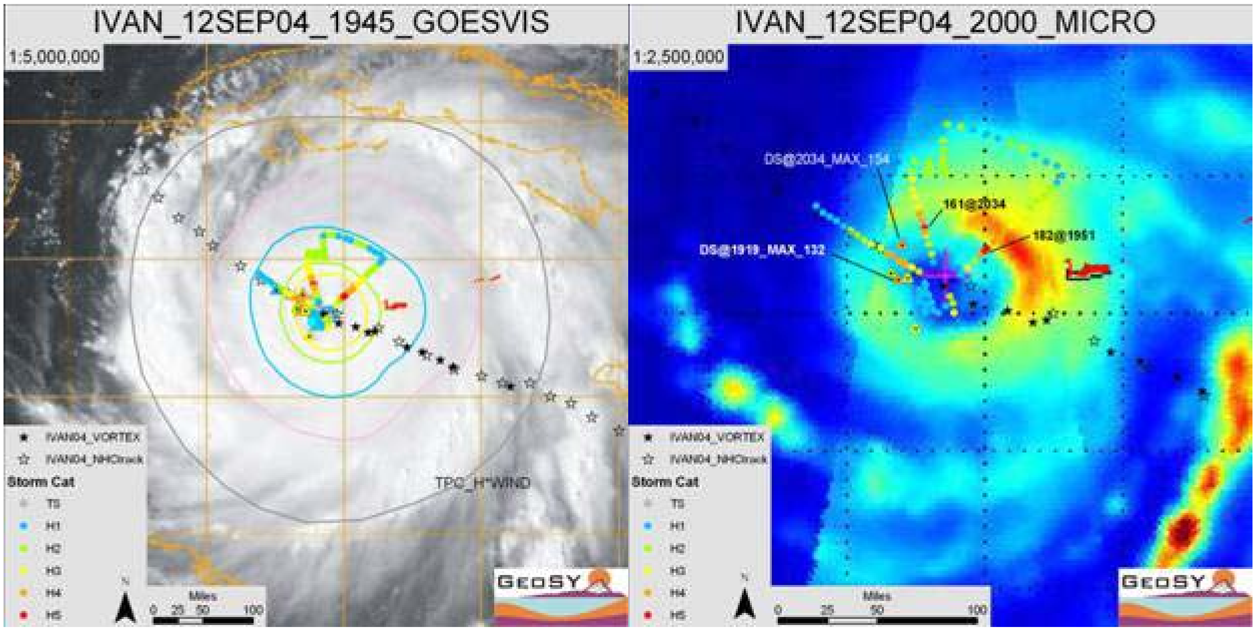

Figure 3.14 GOES visible (left) and morphed microwave (right) imagery for the period around 2000 UTC (3 pm local time) on 12 September. The image at left shows the wind radii from the NHC H*WIND analysis for 1930 UTC. As is clear from the airborne data, the storm intensity is increasing rapidly, with flight level winds in excess of 180 mph and surface winds of 154 mph both from the northern eyewall.

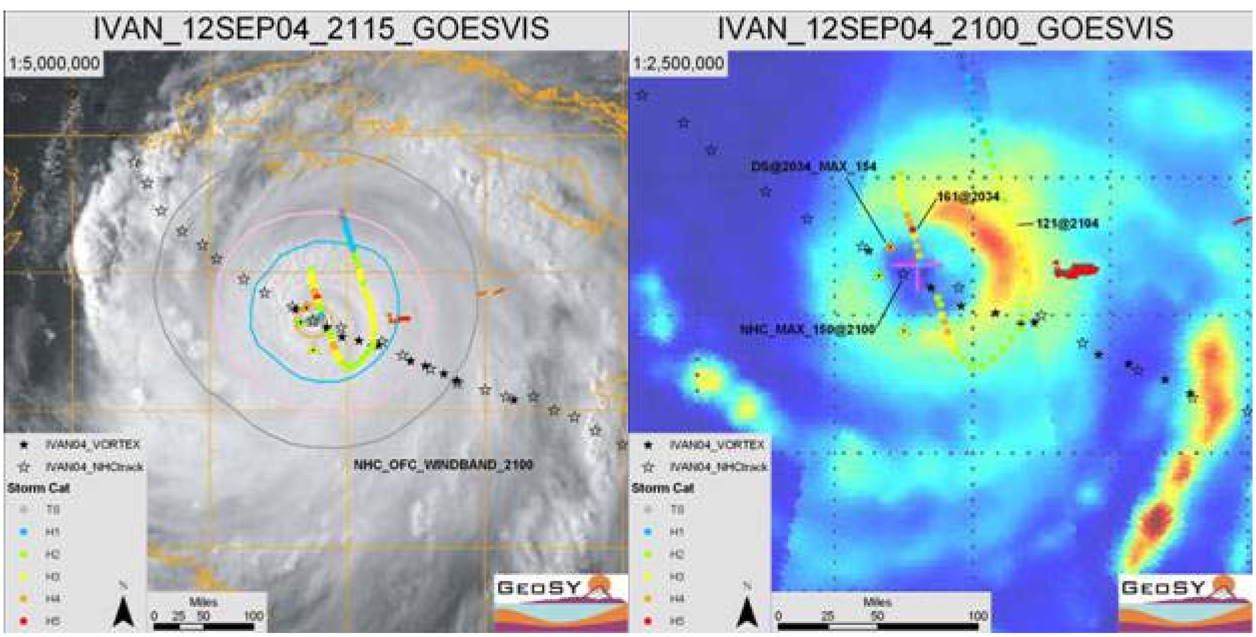

Figure 3.15 GOES visible (left) and morphed microwave (right) imagery for the period around 2100 UTC (4 pm local time) on 12 September. The storm is well to the west of Grand Cayman but with an expanded and intensifying eyewall, hurricane winds are still being felt across the island.

3.3 Best estimates of hazardous phenomena

This section details the best estimate of actual hazardous conditions felt on Grand Cayman for Hurricane Ivan. Using the analysis described above, the wind speed and direction themselves are modelled using the relatively simple approach of Holland (1980) as performed in HurrTrak EMPro (PC Weather Products software). The temporal evolution of surge and wave hazards are controlled by the same model, although surge flooding levels are estimated only from ground-based measurements. Rainfall is obtained from satellite imagery. Both modelled rainfall and wind speed are compared with the scant real-time measurements.

3.3.1 Wind speed and direction

Peak wind speed measurements on Grand Cayman were limited to a single anemometer in West Bay, which recorded a 1-minute sustained wind of 150 mph around 10 am local time on 12 September. The various other reports of peak wind speeds and gusts are not based on actual recordings of wind speed and all can be discounted as unsubstantiated rumour. Figure 3.16 shows the temporal evolution of wind speed from 1pm local on 11 to 7am local on 13 September in 3 locations on Grand Cayman as deduced from the hurricane windfield model described above. For comparison, Mike Whiteman's anemometer data are also plotted.

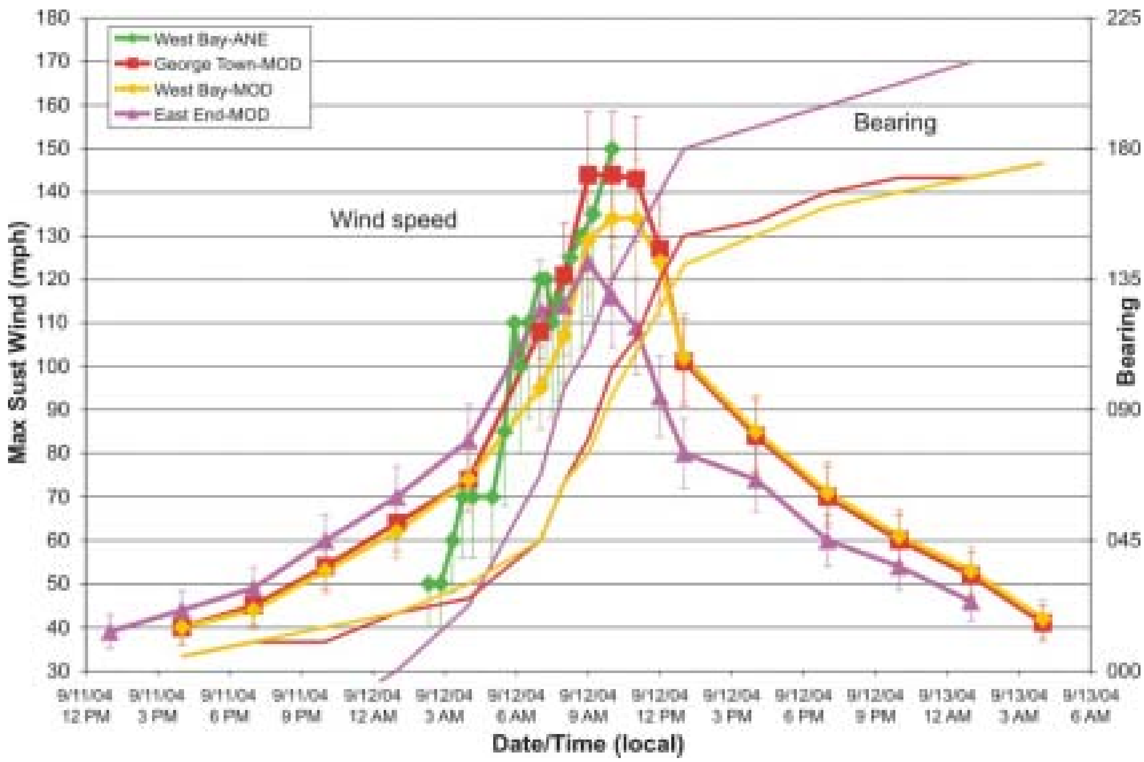

Figure 3.16 Temporal evolution of modelled peak wind speed and bearing for 3 locations on Grand Cayman, and for the anemometer at West Bay. Error bars are ±10% for modelled wind speed and -20% for anemometer wind speed. Time axis is local time.

A tabulation of key data is provided as Table 3.1. The peak wind speed for West Bay from the model is about 10% lower than that recorded by the anemometer; given the likely errors in the anemometer data, this discrepancy is entirely reasonable. The distribution of peak winds across the island is consistent with damage levels on a gross scale (*i.e.* much more damage in the west than the east); however, local conditions related both to perturbations in the windfield and to design and quality of roofing dominate variations in damage on a local scale. All indicators show that peak winds were out of the east across the entire island, and the model is entirely consistent with this observation.

Location	***Peak wind (mph)***	***Peak Gust (mph)***	***Time of peak (local)***	***Time at Cat 3 or above (>110 mph)***
George Town	145	181	9.30 am	7.15 am – 12.35 pm
West Bay	135	169	10.30 am	8.10 am - 12.35 pm
East End	124	155	9.00 am	7 – 11 am

Table 3.1 Key parameters for winds on Grand Cayman during Ivan. Note that the wind model has an error estimated to be ±10%.

Figure 3.17 shows snapshots of the windfield of Ivan at 1500 and 1800 UTC on 12 September and the associated animation shows the full sequence of windfield plots from 1500 UTC on 11 September to 1200 UTC on 13 September.

Key observations from the wind profile data are:

- Category 4 winds were sustained over the George Town area for almost 4 hours, peaking at 140-145 mph between 9 and 11 am local time
- Category 4 winds were sustained in the West Bay area for around 3 hours, peaking at 130-135 mph between 10 and 11 am local time
- Category 3 winds were sustained over the East End area for 4 hours, peaking at 120-125 mph at around 9 am local time
- Using a standard conversion factor, wind gusts likely reached 180 mph over George Town
- Tropical storm force winds (39-73 mph) started in East End at around 1 pm local time on 11 September and ended around 5 am local time on 13 September, a total period of 40 hours. Hurricane force winds (>73 mph) were sustained somewhere on Grand Cayman for almost 18 hours.

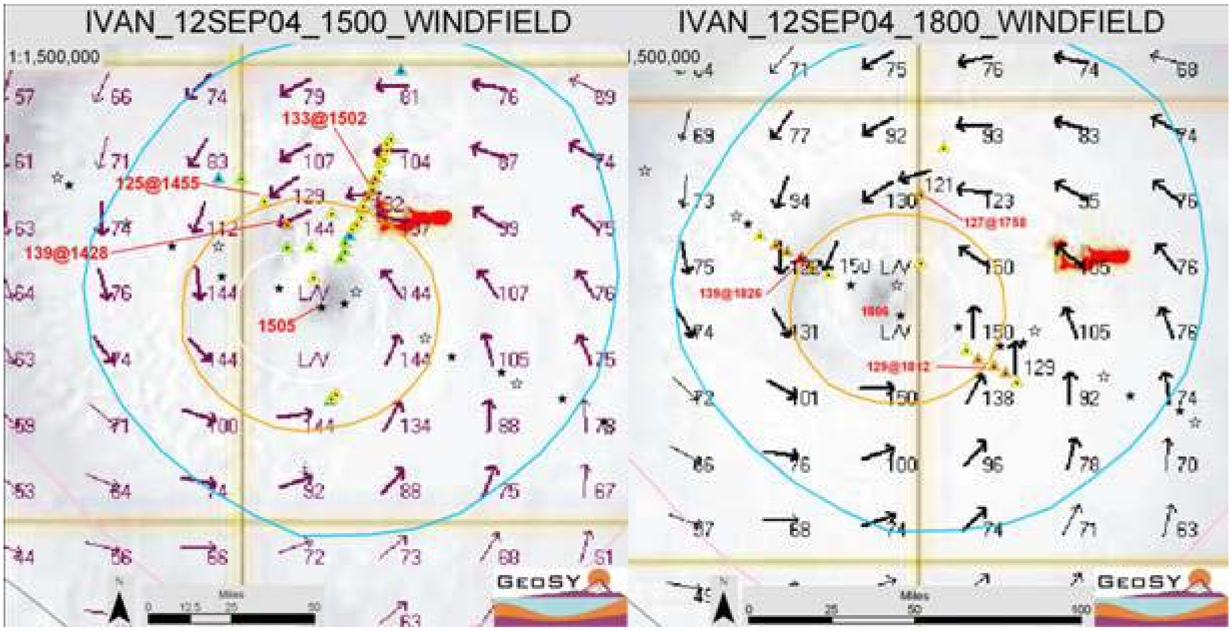

Figure 3.17 Windfield plots superimposed on visible GOES imagery and airborne reconnaissance data (adjusted to surface winds) for 1500 and 1800 UTC on 12 September. The 1500 UTC image depicts near peak conditions in George Town; note the excellent fit of modelled with actual winds for both time windows. Click here to play an animation of the windfield from 1500 UTC on 11 September to 1200 UTC on 13 September.

3.3.2 Rainfall

The Cayman Island's National Weather Service recorded rainfall of 12.1 inches (~300 mm) for Grand Cayman during Ivan (between 0000 UTC on 12 September and 1200 UTC on 14 September). This compares with satellite-based data indicating rainfall of 450-500 mm (18-20 inches) for the same period (Figure 3.18). The discrepancy can be accounted for by the poor accuracy of satellite rainfall measurement techniques and by the inability of rain gauges to accurately record rainfall during strong winds. A reasonable compromise of 15-18 inches (400-450 mm) is provided as the best estimate of total rainfall.

Detailed rainfall rate data were unavailable from ground-based measurement; satellite data indicates peak rainfall of around 1 to 1.2 inches (25-30 mm) per hour for the period between 1400 and 1600 UTC on 12 September (Figure 3.19). Rainfall from Ivan started in Grand Cayman around 1800 UTC on 11 September and cleared around 0000 UTC on 14 September (although there were some further rain showers throughout 14 September.) The animation in Figure 3.19 depicts the changing rainfall rate as Ivan passed Grand Cayman.

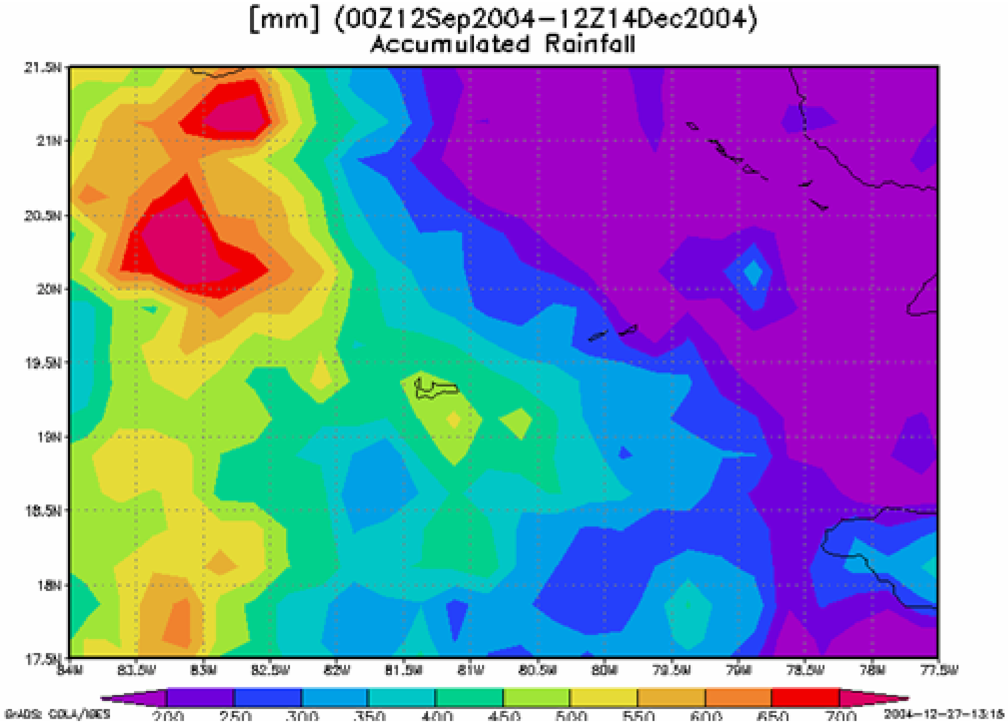

Figure 3.18 Accumulated rainfall for the area around Grand Cayman for the 60 hours from 0000 UTC on 12 September.

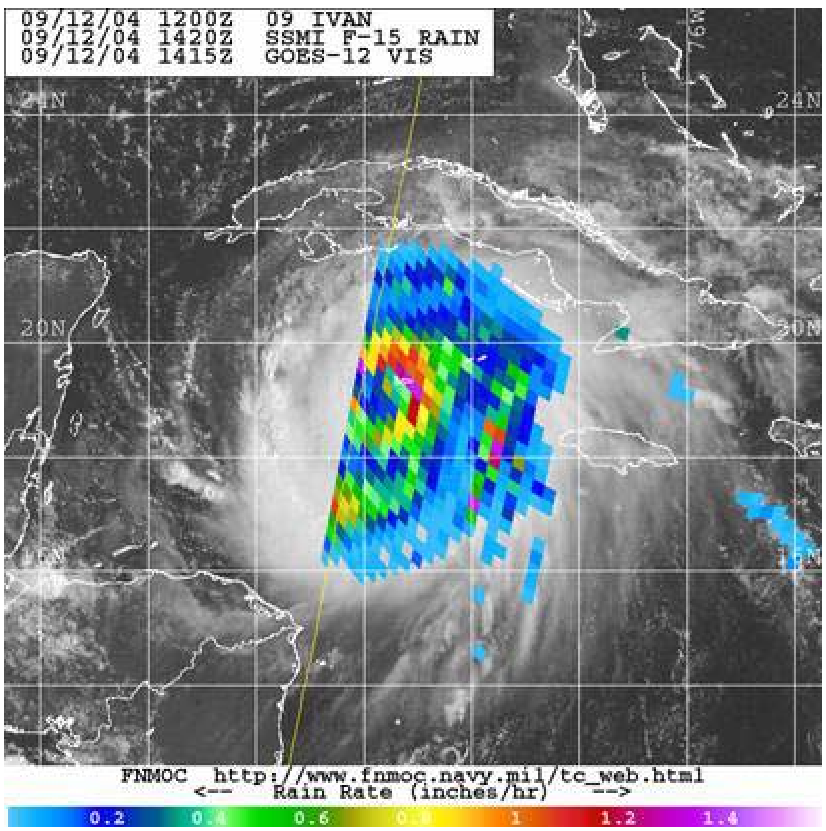

Figure 3.19 Rainfall rate estimated from the SSMI microwave sensor onboard the DMSP-15 satellite. Image at 1420 UTC on 12 September. Click here to play an animation of average hourly rainfall rate (image timed at the end of each 3 hour period) from various microwave sensors for the 54 hour period starting at 1800 on 11 September.

3.3.3 Storm surge and wave action

Both storm surge flooding and wave action were strongly influenced by the evolution of Ivan's windfield as it passed Cayman. While in some respects Grand Cayman was on the bad, northern side of Ivan, there was some good fortune in that onshore winds were not a factor on the most developed, western coastline of the island. Elsewhere, onshore winds produced a storm surge of 6-9 ft and wave heights in excess of 25 ft.

A key, though seldom fully appreciated, aspect of storm surge, important to this case, is that it comprises two distinct elements. The height of storm surge in a particular storm is a function of both a raising of the sea surface induced by low pressure and a frictional pushing of water in the downwind direction, causing a 'stacking up' of water. The conversion of these two basic elements of surge into coastal inundation is further controlled by near-shore bathymetry.

The geometry of North Sound (Figure 3.20) caused the unanticipated, though not unpredicted nor unprecedented, storm surge flooding through the Red Bay-Prospect neck and across the western peninsula. Similar flooding has occurred on a number of occasions in recorded history on Grand Cayman (see next chapter), although the extent of flooding was perhaps greater than on any previously recorded occasion.

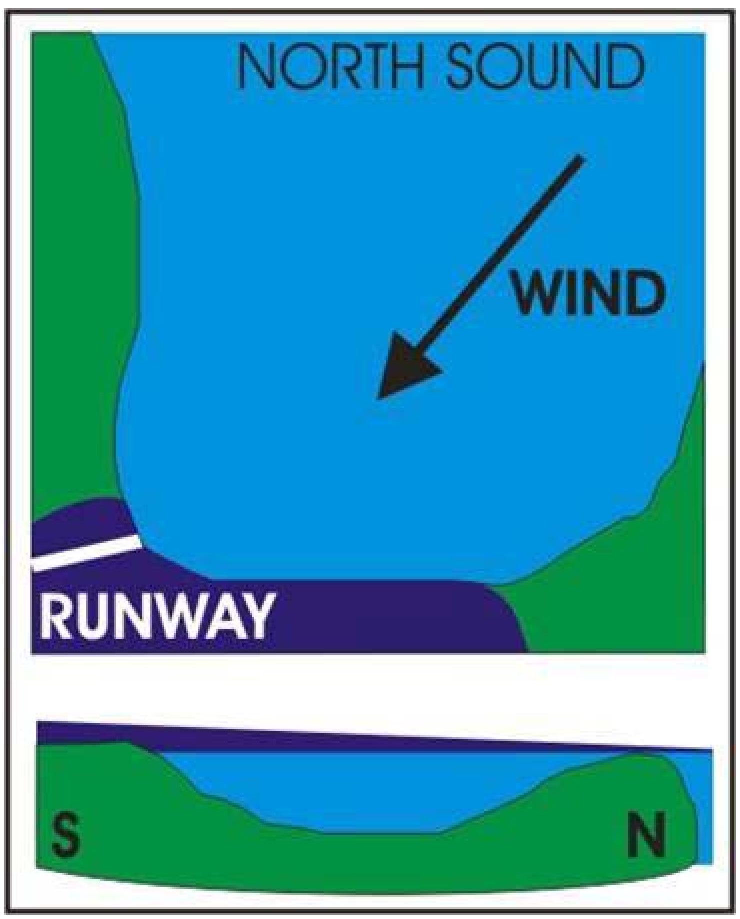

Figure 3.20 Cartoon of the southern part of North Sound in plan (top) and cross-section views. Light blue is the normal water level, dark blue represents the wind-blown surge element.

A key to understanding the unique bathymetry of North Sound and its influence on storm surge is the observation that storm surge flooding in Cayman Kai, seemingly highly exposed at the northern entrance to North Sound, was just 1-2 ft. This proves that there was a substantial slope in the surface of North Sound, up towards the southwest, achieving a height difference of at least 6 ft from northeast to southwest around 6 am on 12 September.

The early northerly and northeasterly winds, though not the strongest, began to push water into the southern parts of North Sound, causing the first extensive flooding (as recorded at the airport) at between 5 and 6 am local time, coincident with the high tide (1.3 ft at 5.22 am). This surge flooding receded quickly as the tide turned. As the winds swung around to the east, water began to inundate the western shore of North Sound and, in places, pushed right across the western peninsula to Seven Mile Beach. At the peak of the storm, between 9 and 11 am on 12 September, easterly winds over western Grand Cayman and southeasterly winds over eastern Grand Cayman (see Figure 3.17) caused storm surge inundation from both the western side of North Sound and from South Sound simultaneously. The main storm surge flooding peak was recorded along South Sound at around 11 am, likely the result of winds having swung to onshore in that area. The continued onshore winds at South Sound prevented draining of flood waters until the late afternoon; backflow into North Sound occurred somewhat earlier than that, although southerly winds prevented draining of water over Seven Mile Beach late into the evening.

During this project, there was insufficient time to collect and process a fully representative set of water height estimates. It is recommended that personal memories and actual measurements are collected systematically on Grand Cayman so that a fuller picture of flood levels can be gathered. Table 3.2 summarises a few key measurements of water height during the surge-induced flooding.

Location	***Depth of flooding (inches)***	***Height of floor (ft amsl)***	***Flood height (ft amsl)***
Met Office, Airport	18	7	8.5
Grand Caymanian, Welch Point	24	4	6
Bayshore Drive, The Shores	18	8	9.5
Secret Gardens, South Sound	45	4	8
Bodden Town Police Station	12	6	7
Cayman Kai	12	2	3

Table 3.2 Summary of surge-induced flood heights. Note that floor heights, and thus total flood heights, are approximations only. Accurate elevation data is required to better constrain these numbers.

Storm surge flooding, although damaging, is somewhat of a passive process. Water levels tend to rise relatively slowly (although true ‘surges’ of water certainly do occur, usually related to surge height reaching above key retaining structures), and damage is done not through active erosion but by everything getting wet. Several cases were noted on Grand Cayman where rising or falling flood water along a confined area caused significant erosion and damage but, in general, erosional water damage was caused by wave action.

Wave damage along the coast of Grand Cayman was highly variable in its nature. The variability in damage levels was entirely controlled by the presence or absence of shallow offshore coral reefs and the presence or absence of onshore winds during the storm. Waves break in shallowing water; even with the storm surge, the reefs which surround most of the south, east and north coast of Grand Cayman were sufficiently shallow to cause waves to break, thus dissipating almost all of their energy. The relatively unprotected west coast was fortunately not subject to onshore winds. Thus severe wave damage occurred only in a few places where onshore winds and no shallow reef protection came together. These areas are shown in Figure 3.21.

The east-facing coast of North Sound is in the process of being developed; this area received minor wave damage from water driven across the longest reach of North Sound during the peak of the storm. High Rock has a history of exposure to strong waves once winds are out of the southeast; large boulders at ~30 ft above sea level were reportedly carried there during the 1932 hurricane. In this area, houses ~25 ft above sea level received extensive wave damage. At Ocean Club/Mariner’s Cove, onshore winds came around 11 am on 12 September and quickly devastated these two resorts. They had no protection from either reefs or from any significant height above sea level. Wave heights here were probably lower than at High Rock, with erosion by waves occurring up to about 15 ft above sea level. The final area of damage was on the south-facing stretch of West Bay, where onshore winds late in the storm drove waves into Dolphin Point and other resorts in this area, causing widespread damage. Estimated wave heights here were 10-15 ft.

As previously mentioned, the main stretch of developed coastline, and Grand Cayman’s primary tourist attraction, is the west-facing Seven Mile Beach. The west coast of the island has no shallow reef protection, and strong onshore winds during future storms may cause much more extensive damage from wave action than resulted from storm surge flooding on this occasion.

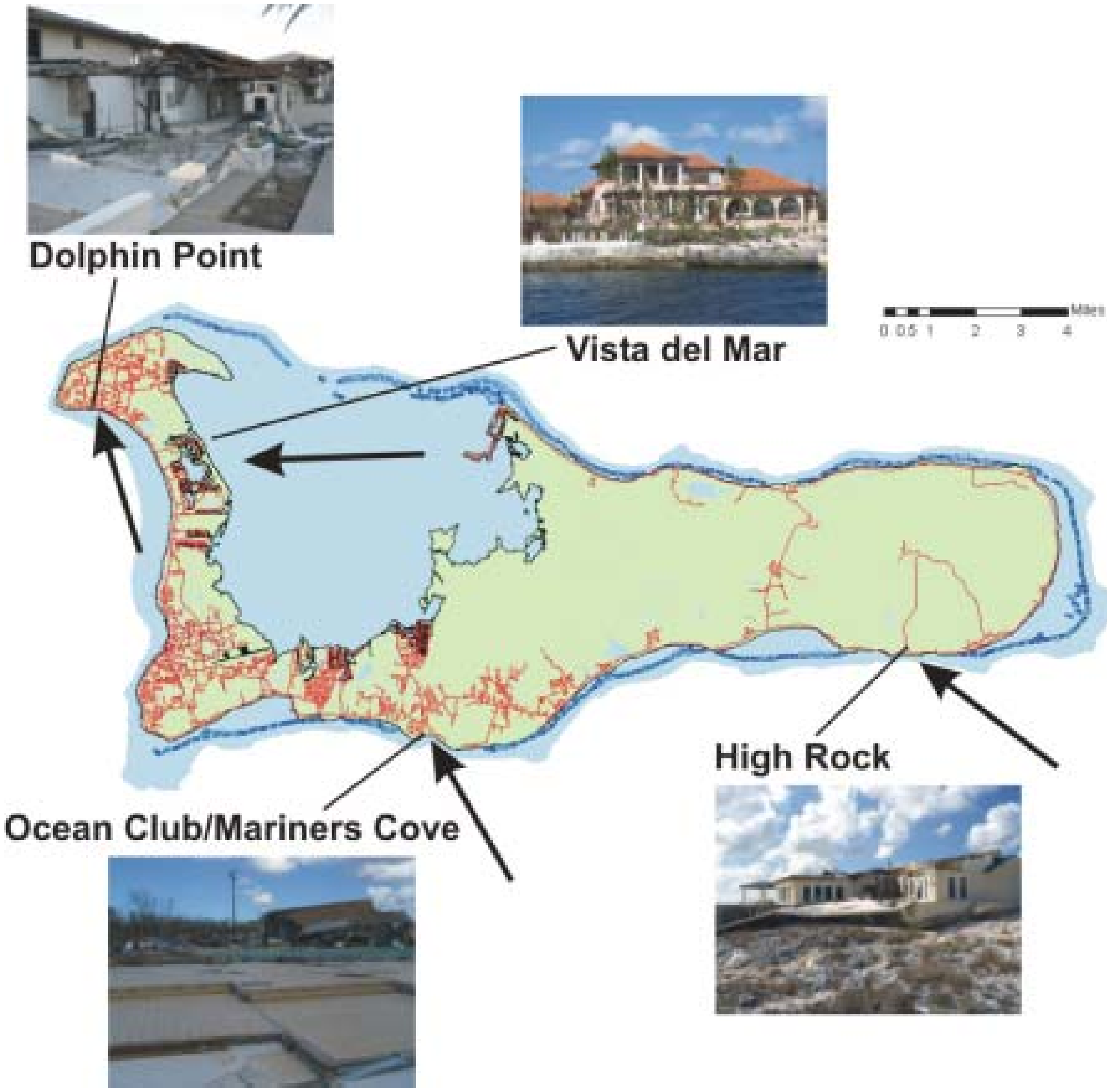

Figure 3.21 Key elements of wave damage around the coast of Grand Cayman. Large arrows indicate wind direction when damage was initiated.

4 COMPARING FORECASTS AND HAZARD MODELS TO REALITY

This chapter assesses the adequacy of both short term, real-time forecasts on the basis of which emergency management decisions were taken and long term, probabilistic-type forecasts on the basis of which development planning decisions are taken.

Short term forecasts, issued by the National Hurricane Center in Miami, have improved dramatically over the past decade or so, and this rapid improvement is likely to slow substantially as forecasting approaches the limit of its powers. It is unlikely that substantial further reduction in forecasting errors will be achieved in the coming years; therefore the assessment presented in section 4.1 provides a basis on which the inherent uncertainties in hurricane forecasting can be integrated into emergency management planning and decision-making.

Section 4.2 presents a brief review of the performance of the TAOS model in its real-time guise as a risk analysis tool. TAOS (The Arbiter Of Storms) was developed by Charles Watson of Kinetic Analysis Corp. under the auspices of the Organisation of American States (OAS) managed Caribbean Disaster Management Project (CDMP). It currently stands as the only public-domain real-time hazard and risk analysis tool for the region (OAS, 1999).

Long-term forecasting for Grand Cayman, in the form of probabilistic hurricane hazard analysis, has substantial room for improvement, and improved maps may have key implications for development planning in the Cayman Islands. Although the occurrence of a ‘rare’ storm does not invalidate probabilistic assessments of the likelihood of such events, some of the consequences of the ‘rare’ storm appear to have been significantly underestimated in previous hazards assessments for the Cayman Islands. Section 4.3 presents an analysis of the two quantitative, model-based studies available, from CDMP (via TAOS model) and from a Cayman PWD-commissioned study. Section 4.4 presents a semi-quantitative assessment of hurricane hazards from the historical record.

4.1 Short term forecasting

Analysis of the NHC forecasts for Ivan suggests that they were of moderate accuracy for most of its track across the Caribbean Sea, though for the 12 hour period in which Grand Cayman was most severely affected, the forecasts were actually better than for most of the previous 10 days.

Figure 4.1 shows the position error on all NHC forecasts from 3 September through to 14 September. The time at the bottom is the time for which the forecast was made, and the different forecast periods are shown in different colours. The grey band represents the in which Grand Cayman was most severely affected.

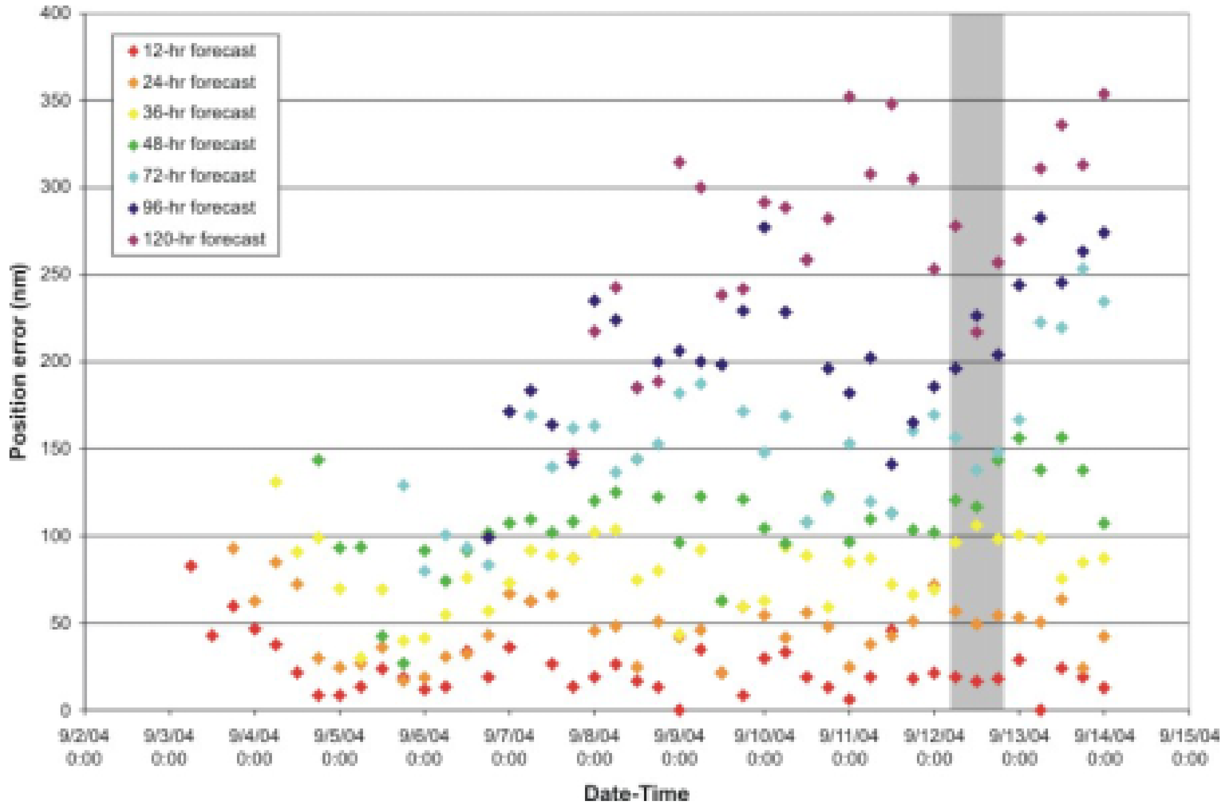

Figure 4.1 Position errors of NHC official forecasts for Hurricane Ivan during its passage across the western Atlantic and Caribbean Sea.

For the period between 0300 and 2100 on 12 September, the average forecast position error was around 60nm/day. The key forecast times for the emergency management preparation activities in the Cayman Islands are those at 48 hours (Alert level), 36 hours (Watch level) and 24 hours (Warning level). For those time periods specifically, the position errors averaged 127 nm, 100 nm and 53 nm.

Figure 4.2 is a plot of the intensity errors for the same time period. As is clear from the scattered nature of the data on this plot, intensity forecasting is much more difficult than track forecasting, and the largest intensity errors are induced by rapid intensification cycles. In terms of the specific forecasting for Ivan in Cayman, its passage at a temporarily reduced intensity meant that the forecasts were pretty good. For the key forecast times at 48, 36 and 24 hours, the average intensity errors for Ivan were -7, -2 and +3 kt (negative meaning that the forecast overestimated the intensity).

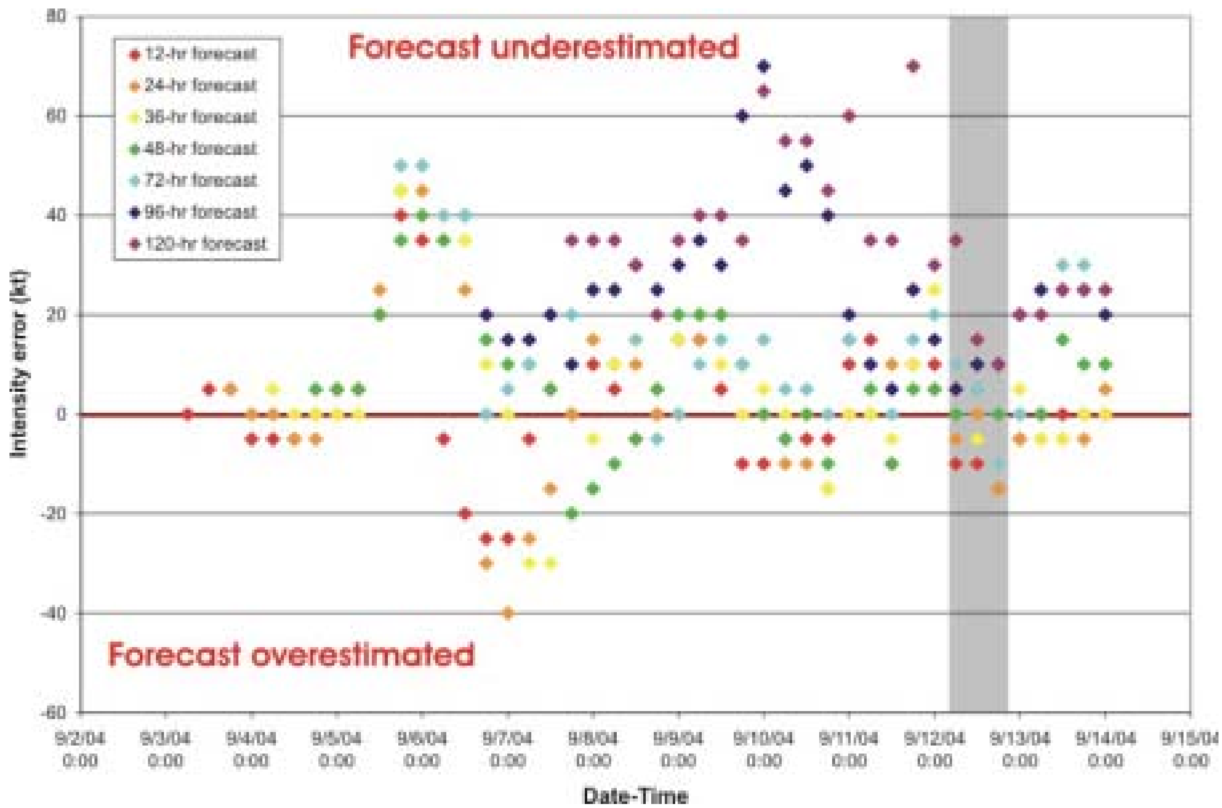

Figure 4.2 Intensity errors of NHC official forecasts for Hurricane Ivan during its passage across the western Atlantic and Caribbean Sea.

As an illustration of what these forecast errors mean in reality, Table 4.1 shows the range of possible peak conditions in Grand Cayman from Ivan based on the 48, 36 and 24 hour forecast errors described above.

	Actual	*48-hr forecast*	*36-hr forecast*	*24-hr forecast*
Position (1200 UTC)	18.8N, 81.2W	20.5N, 80.2W	20.4N, 80.4W	19.6N, 81.0W
Intensity (1200 UTC)	135 kt	125 kt	140 kt	135 kt
Best case wind George Town	144 mph	< 39 mph	<39 mph	60 mph
Worst case wind George Town	144 mph	152 mph	163 mph	159 mph

Table 4.1 Illustration of the range of peak wind conditions which were ‘predicted’ from the NHC forecasts, using calculated errors, at 48, 36 and 24 hours averaged for the period 0300-2100 UTC on 12 September.

As can be seen from Table 4.1, even with 24 hours notice, the range of possible wind speeds which could have, within the error of the forecast, affected George Town was huge, from 60 mph (which would have caused almost no wind damage) to 160 mph, which would have been catastrophic. Similar ranges in storm surge and wave action are likely, although time constraints have limited the ability to model these phenomena.

4.2 TAOS real-time modelling of hazardous phenomena

The TAOS system, developed under the auspices of CDMP, is available via a web-based interface for real time hazard (and, to a limited degree, risk) assessment in the Caribbean (and, in fact, globally). The real time forward modelling is done on the basis of the forecast track and intensity data; errors in the modelling in this case are probably small compared to the forecast errors, highlighted in the previous section. In this section, a brief assessment of the post-hoc TAOS model run for Ivan is presented. Note that this post-hoc run uses the official track data rather than the most recently published best track data; the use of the updated best track would make negligible difference to the analysis presented here.

TAOS on the web provides options to plot wind field, storm surge and rainfall accumulation and, for the area of the Cayman Islands, these plots are provided in Figures 4.3 and 4.4 for Ivan.

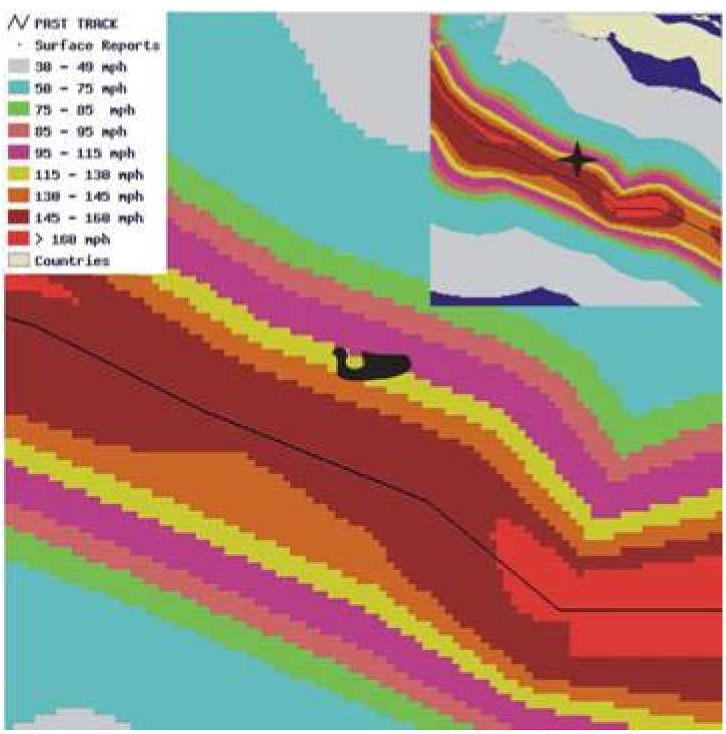

Figure 4.3 Windfield model from TAOS for Ivan. Inset is wide-area map.

Figure 4.4 Storm surge height and accumulated rainfall estimation from TAOS model for Ivan.

It is clear from these plots that the TAOS model significantly underestimated all of the hazardous phenomena encountered on Grand Cayman during the passage of Ivan. Peak wind speeds are projected to be 130-135 mph for the southwest corner of the island and 115-130 for most of the rest of the island. This represents a 7-10% underestimate. This underestimate is almost certainly due to the assumption in the model of a 'normal' eye structure for Ivan at this time; the analysis presented earlier shows a significantly expanded eye and eyewall at the time of Ivan's passage past Grand Cayman.

Storm surge height is badly underestimated, likely due to low resolution bathymetric control in the TAOS model. The storm surge model appears to be representative only for Cayman Kai and perhaps some areas of the north coast, but completely misses the important effect of windblown water from both North and South Sound.

The rainfall total is also a significant underestimation, being less than one third of what actually fell. The details of rainfall estimation in TAOS are unknown, so the source of this major discrepancy cannot be ascertained.

In general then, the TAOS model in this case did not perform very well and, if used in its forward modelling mode using forecasts as input, then the output from the model would not have been, in this case, useful. A further discussion of the use of forward modelling for approaching storms is provided in the next chapter.

4.3 Long term forecasting – modelling approach

Two quantitative hazard assessment studies for tropical cyclone effects have been located for the Cayman Islands. One, undertaken as part of the CDMP-TAOS hazard mapping effort, includes Cayman only as a bi-product; a detailed atlas for the CDERA member states was produced and widely distributed but the Cayman area only appears on regional maps which are not readily available. It has not been ascertained whether or not these maps are actually in the possession of the relevant authorities in Cayman. The second study was undertaken by a consultant for the Public Works Department of the Cayman Islands Government (Minor & Murphy, 1999); again, the circulation reach of this report within Government circles is unknown.

The TAOS study produced probabilistic hazard maps for wind, surge and wave height for return periods of 10, 25, 50 and 100 years, based on the modelled effects of 150 years worth of Atlantic storms and some statistical analysis. Figure 4.5 shows two wind hazard maps; a 50% probability of exceedance in 50 year map and a 50% probability of exceedance in 100 year map. The first of these maps is directly analogous to the level of hazard referred to in seismic engineering as the 'maximum probable earthquake'. The second most closely resembles the windfield encountered during Hurricane Ivan.

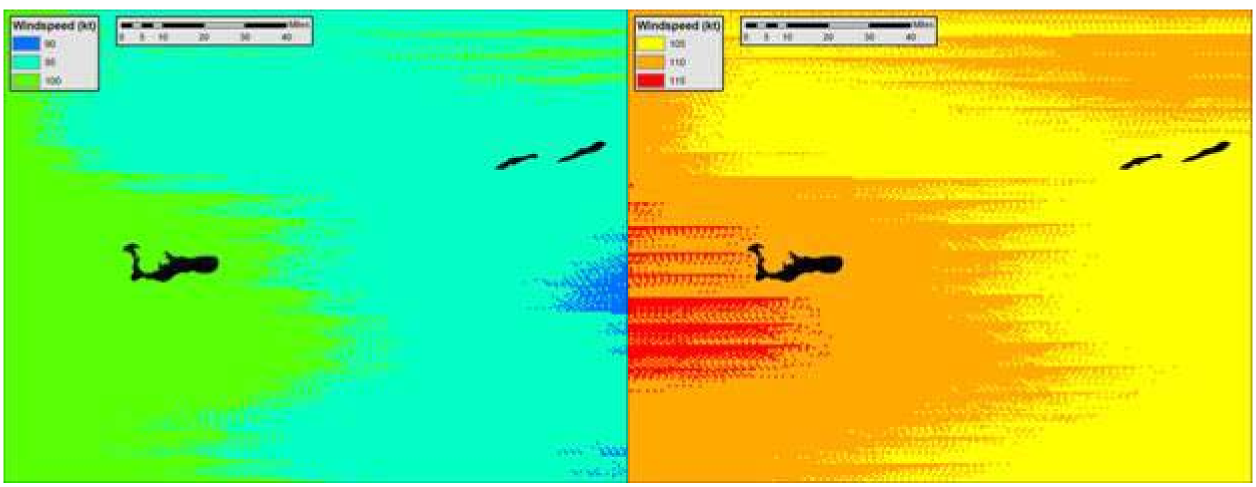

Figure 4.5 Probabilistic wind hazard maps at 50 year (left) and 100 year (right) return periods for Cayman from TAOS-CDMP.

Comparison of these probabilistic maps with the actual windfield of Ivan suggests that, for winds at least, Ivan was a little worse than a 'once in 100 year' storm.

Figure 4.6 shows equivalent plots for storm surge and Figure 4.7 for wave heights. As with the 'real-time' TAOS output discussed in the previous section, the storm surge estimate (relative to the wind speed at least) is significantly lower than was actually encountered. Wave height estimation appears to be reasonable.

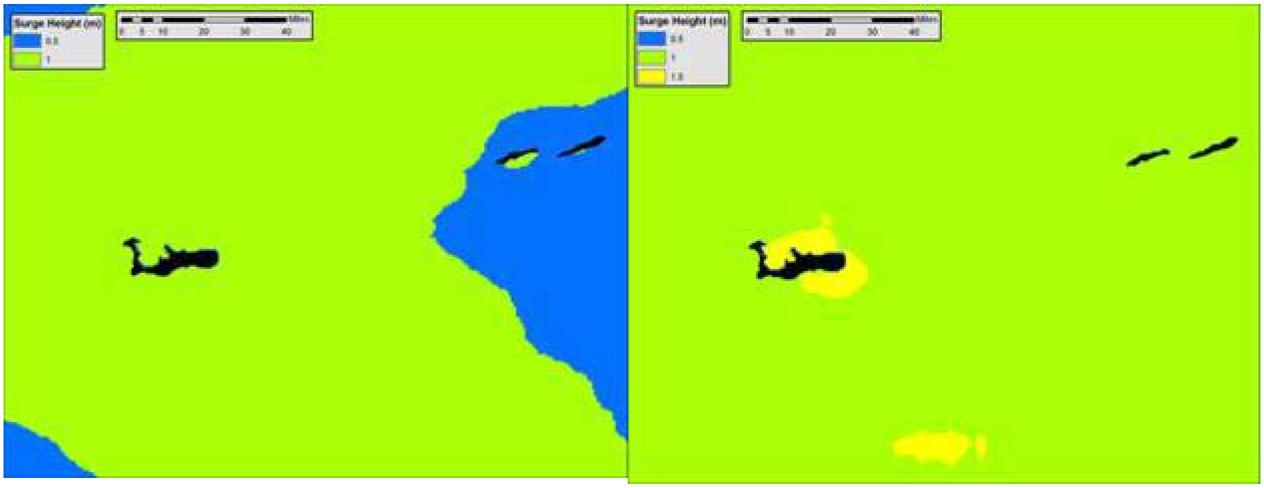

Figure 4.6 Probabilistic storm surge hazard maps at 50 year (left) and 100 year (right) return periods for Cayman from TAOS-CDMP.

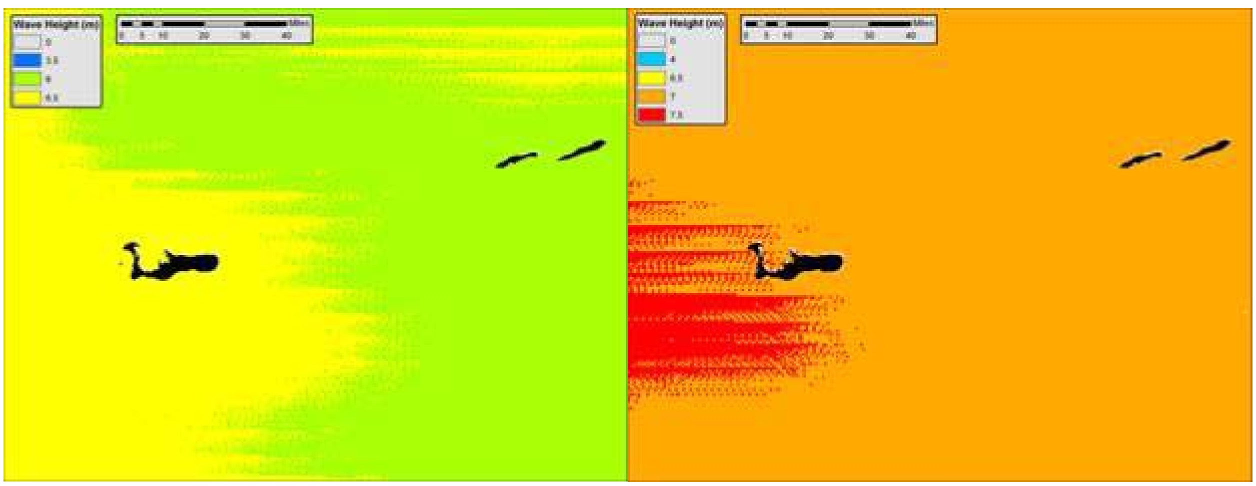

Figure 4.7 Probabilistic wave height hazard maps at 50 year (left) and 100 year (right) return periods for Cayman from TAOS-CDMP.

In this case the surge hazard map does appear to model the surge in North Sound a little better than the specific output from TAOS for Ivan, but the surge model is still clearly inadequate to adequately quantify the surge hazard for Cayman. The wave model, although giving the right general level of wave hazards, is not sufficiently detailed to represent potential for wave damage which, as previously described, is highly dependent on the presence of absence of offshore reefs.

The report for PWD draws on, for wind hazards at least, the hurricane hazard model of Applied Research Associates (ARA). This model is similar, in principal, to the TAOS model, although there are fundamental differences in the detail of the model. The summary output for Grand Cayman from the ARA wind model is reproduced in Table 4.2.

Return Period	*Peak 1-min sustained (mph)*	*Peak 3-sec gust (mph)*
10	59	75
50	91	115
100	105	134
500	130	166
1000	141	180
2000	154	196

Table 4.2 ARA modelled tropical cyclone peak sustained and gust winds for Grand Cayman at various return periods.

As is clear, for wind speed at least, the ARA model varies significantly from the TAOS model, with Ivan on this basis a little worse than a 'once in 1,000 year' storm.

No quantitative data on surge and wave hazard is presented in the PWD report; however, there is a qualitative description of the possible amplification effect of North Sound on surge heights and of the potential for lack of offshore reefs to cause waves to crash at the shoreline.

4.4 Historical perspective

Given the major discrepancies in the wind hazard modelling approaches described above, and the lack of credible information regarding surge and wave hazards, this section reviews the historical record for Cayman to try to get another perspective. The historical assessment includes both written evidence for historical impacts in the Cayman Islands and a simple model which assesses likely wind fields for historical hurricanes passing close to Cayman.

4.4.1 Written history

Table 4.3 presents a list of historical hurricanes for which there is some information available which might help assess the level of hazardous phenomena encountered on Grand Cayman at the time. This list is taken from an article written by Carol Winker of Cayman Free Press, based on multiple historical records. The table also includes the estimated wind speed, based on a simple wind field model run by the author and described in the next section.

Year	*Wind description*	*Surge/wave description*	*Est. peak wind (mph)*
1731		Breach at Newlands	
1751		Breach at Pedro	
1785	Appears very severe	Appears very severe	
1837/38	Two severe storms		
1846		Major breach through Newlands	
1876	Appears severe		72
1903	Severe but short	Seas not bad	120
1915		Breach at Spotts	64
1915		Worst since 1846	57
1932	Worst ever	Major breaches, rocks at High Rock	67
1933		Breach at Prospect	50
1944		Breach at Red Bay/Prospect	90
1988	Gilbert – gusts to 135mph	Breaches at Red Bay/Pedro	107

Table 4.3 Key historical storms and hazardous phenomena for Grand Cayman.

In the 270 years or so of hurricane history available (although prior to 1850 or so, there may be information missing), there have been at least 10 occasions where storm surge has breached the island, probably in a similar manor (but not necessarily as severely) as during Ivan. There is also evidence for strong wave action during storms in the areas not protected by reefs; accounts of large rocks found about 30 ft above sea level at High Rock suggest that they were put there by waves during the 1932 storm, indicating that it was probably more severe, in terms of its surge and wave damage, than Ivan.

4.4.2 Simple wind modelling

Even semi-quantitative information regarding peak wind speeds is difficult to ascertain from the historical record; however, for the period since 1851, the NOAA best track hurricane database can be used, along with a simple windfield model, to estimate the peak winds during storms passing close to Grand Cayman. The simple model employed by the author uses the windfield data from NHC for the past 14 years of storms in the northwestern Caribbean Sea to calculate wind speeds on Grand Cayman for all previous storms for which hurricane force winds were likely to have been encountered. The output from the simple model is accurate to within 10-15%, the error being induced by assuming an average windfield and eyewall profile.

The results of the simple windfield modelling are summarised below. Hurricane Ivan comes out as the most intense storm in terms of felt wind speed on Grand Cayman; the simple model underestimates the actual wind speed in Ivan by a little less than 15%. The only other two storms with estimated winds of over 100 mph on Grand Cayman were Gilbert in 1988 (estimated 107 mph) and a storm in August 1903 (120 mph). The 1903 storm is interesting in that it does not appear in historical records to have been a particularly severe event, even though it went directly over the middle of Grand Cayman with estimated intensity of 120 mph (from the NOAA best track database.) The historical record actually suggests that the sea conditions for this storm were very mild.

Only three other storms appear to have produced hurricane force winds on Grand Cayman; a November storm in 1912, a September storm in 1948 and the October storm in 1944 which is in Table 4.3 There appears to be no historical documentation of the 1912 and 1948 storms.

A further 21 storms had estimated winds from the simple model of 65 mph or greater, within the error margin of the model. If, say, half of these storms produced hurricane winds on Grand Cayman then there would have been a total of 16 storms producing hurricane force winds in Grand Cayman since 1851, one every 9.6 years. Severe storms, with winds greater than 110 mph, are much rarer, with only two having occurred in the same period (one every 77 years, on average).

Comparing these results to the ARA model results, we can see that the ARA model appears to underestimate the wind hazard on Grand Cayman; its 10-year return period wind is only 60 mph and its 77-year return period wind is only around 98 mph. In contrast, the TAOS modelled winds for 77-year return period is 109 mph.

In conclusion, the wind models suggest that Ivan’s winds were a 1 in 100 to 1 in 200 year event. The storm surge and wave action were probably a little less rare than that, perhaps a 1 in 50 to 1 in 100 year event. Even though these events are thus quite rare, Ivan does not represent a worst-case scenario for Grand Cayman. A storm passing across the eastern side of the island would produce the strongest winds blowing onshore at Seven Mile Beach; without reef protection, surge and especially wave damage could be far more destructive, given the value of property at risk, than was Ivan’s.

It should be noted that this historical analysis applies only to Grand Cayman; some of the storms listed in Table 4.3, and some additional storms, certainly produced worse conditions on the sister islands to the east than on Grand Cayman. The November 1932 storm is a good case in point; even though it had some severe impacts in Grand Cayman, the sister islands were much more severely hit on that occasion.

5 CONCLUSIONS AND RECOMMENDATIONS

This chapter briefly discusses the conclusions of this study and recommendations specifically in the area of improved data collection. A more comprehensive summary and recommendations are provided in the companion summary report for the project.

5.1 Conclusions

Hurricane Ivan was an unusually strong hurricane which produced high winds, storm surge flooding, heavy rain and strong wave action on Grand Cayman. Ivan was sustained as a severe hurricane throughout its passage across the Caribbean Sea; for all seven days of its Caribbean life, Ivan had peak winds in excess of 130 mph. Few hurricanes sustain such intensity for so long, and none has done so with such a southerly track since reasonable records began 150 years ago.

The impact of Ivan on Grand Cayman was just short of catastrophic. However, this study shows that the meteorological conditions encountered were certainly capable of causing catastrophe, and it was only because of the high standard of built infrastructure, especially shelter accommodation and other critical infrastructure, that loss of life and injuries were kept so low.

Although wind speeds were sustained at 130-145 mph across much of western Grand Cayman for several hours, it was water that did most damage, in the form of storm surge flooding (aided somewhat by heavy rain) and wave action in exposed coastal areas. Although water damage appeared to have come as something of a surprise to many residents of Grand Cayman, the conditions were not unusual for such a strong hurricane and, in fact, there is evidence to suggest that the extent of flooding and wave damage was not as unusual as the ferocity of the winds.

Analysis of the short term forecasting for Ivan and of the few hazard assessments for Grand Cayman suggest that neither performed very well for Ivan. The conditions of wind encountered in Ivan were within the limits of the uncertainty in the forecasts for all time periods, but those uncertainties gave a range of possible peak windspeeds, even at 24 hours notice, of almost 100 mph. This translates to projected damage levels covering the entire range from no damage to severe damage to most infrastructure.

The different probabilistic models cannot be assessed on the basis of one storm, but there are clearly major differences and problems in model performance, and these must be addressed and resolved, and improvements made in surge modelling, for the hazard assessments to be regarded as useful. The results of this project will serve as a useful data set for verification of future hazards studies.

It appears, on the balance of evidence, that Ivan was about a once in 100 year storm. Wind speeds were a little stronger and surge/wave impact perhaps a little less than that, but overall, the impact was probably that of a 100-year event. However, it should be noted that, firstly, two 100-year hurricanes can occur in successive years; the fact that Ivan occurred in 2004 does not give Grand Cayman a guaranteed 99 years without a similar storm, and secondly, that Ivan was somewhat short of a worst case scenario for Grand Cayman.

The socio-economic impacts of Ivan have been very severe, and perhaps have added to the local perception that Ivan was as bad as it is going to get or has ever been on Grand Cayman. The evidence suggests that this is not the case, and that the severe economic impact especially is due mainly to the phenomenal growth in population and infrastructure at risk in Grand Cayman. That population growth has been housed, both residentially and commercially, in well-built structures which generally stood up well to the wind, but were within 10 ft of sea level and thus prone to some degree of flooding. Without a comprehensive revision of building practice for low-lying areas, it is difficult to see how storm surge flooding can be effectively mitigated. In contrast, wave damage occurred only in a few exposed locations, where action could be taken to ensure better structures (or no structures at all) in these areas.

One major issue to come out of this study is the possibility of severe wave damage to the exposed west coast of Grand Cayman during a storm tracking over the eastern side of the island. Even a milder storm than Ivan, if taking such a track, could cause severe wave damage as well as surge flooding along Seven Mile Beach and in George Town. Any future hazard assessment work commissioned for the Cayman Islands should include a specific element looking at worst-case scenario storms.

5.2 Recommendations

The following recommendations are specific to the aspects of this project covered in this report. They are covered in additional detail in the project summary report.

- Hardening of meteorological instrumentation and broadening of the data gathering network to include multiple wind sensors, rain gauges and barometers and initiation of offshore and coastal tide/surge monitoring through fixed tide gauges and ocean-bottom pressure sensors.

- Comprehensive hazard assessment of the Cayman Islands for tropical cyclones, with particular emphasis on storm surge and wave action. Such a study must be of sufficiently high resolution so as to be able to model variations of surge and wave action on the scale of tens of metres, and also must meet a standard of being able to accurately model the impacts of Hurricane Ivan.

- Discussion of large scale, long term development programmes to enable better resistance to storm surge flooding and the damage it produces.

- Continuation of local data gathering, especially of flood levels, to better constrain the surge flooding event.

This page intentionally left blank

6 REFERENCES

Holland, G J. 1980. An analytic model of the wind and pressure profiles in hurricanes. *Monthly Weather Review*, **108**, 1212-1218.

Landsea, C W, Franklin, J L, McAdie, C J, Beven, J L, Gross, J M, Jarvinen, B R, Pasch, R J, Rappaport, E N, Dunion, J P and Dodge, P P. 2004. A Reanalysis of Hurricane Andrew's Intensity. *Bulletin of the American Meteorological Society*, **85 (11)**, 1699–1712.

Minor, J E & Murphy, P. 1999. *The hurricane risk for the Cayman Islands, British West Indies*. Technical Brief to CIG Public Works Department.

Organisation of American States. 1999. Caribbean Disaster Management Project, Final CD-ROM.

Powell M D, Houston, S H & Reinhold, T A. 1996. Hurricane Andrew's Landfall in South Florida. Part I: Standardizing Measurements for Documentation of Surface Wind Fields. *Weather and Forecasting*, **11**, 304-328.